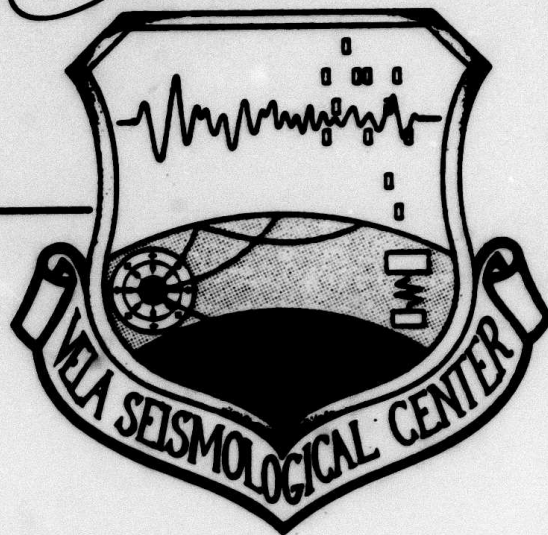


AD A121718

(12)

VSC-TR-82-25

**GROUND MOTION PREDICTIONS FOR
THE GRAND SALINE EXPERIMENT**



N. Rimer
J. T. Cherry

S-CUBED
P.O. Box 1620
La Jolla, California 92038

TOPICAL REPORT

July 1982

**Approved for Public Release,
Distribution Unlimited**

DTIC
ELECTE
NOV 22 1982
A

Monitored by:

VELA Seismological Center
312 Montgomery Street
Alexandria, Virginia 22314

DTIC FILE COPY

82 11 22 108

Unclassified

SECURITY CLASSIFICATION OF THIS PAGE (When Data Entered)

REPORT DOCUMENTATION PAGE		READ INSTRUCTIONS BEFORE COMPLETING FORM
1. REPORT NUMBER VSC-TR-82-25	2. GOVT ACCESSION NO. AD-A121 718	3. RECIPIENT'S CATALOG NUMBER
4. TITLE (and Subtitle) Ground Motion Predictions for the Grand Saline Experiment		5. TYPE OF REPORT & PERIOD COVERED Topical Report (Draft)
		6. PERFORMING ORG. REPORT NUMBER SSS-R-82-5673
7. AUTHOR(s) N. Rimer and J. Theodore Cherry		8. CONTRACT OR GRANT NUMBER(s) F08606-79-C-0008
9. PERFORMING ORGANIZATION NAME AND ADDRESS S-CUBED P.O. Box 1620 La Jolla, California 92038		10. PROGRAM ELEMENT, PROJECT, TASK AREA & WORK UNIT NUMBERS Program Code No. 6H189 ARPA Order No. 2551
11. CONTROLLING OFFICE NAME AND ADDRESS VELA Seismological Center 312 Montgomery Street Alexandria, Virginia 22314		12. REPORT DATE July 1982
		13. NUMBER OF PAGES 64
14. MONITORING AGENCY NAME & ADDRESS (if different from Controlling Office)		15. SECURITY CLASS. (of this report) Unclassified
		15a. DECLASSIFICATION/DOWNGRADING SCHEDULE
16. DISTRIBUTION STATEMENT (of this Report) Approved for Public Release, Distribution Unlimited.		
17. DISTRIBUTION STATEMENT (of the abstract entered in Block 20, if different from Report)		
18. SUPPLEMENTARY NOTES		
19. KEY WORDS (Continue on reverse side if necessary and identify by block number) Ground Motion Seismic Coupling Salt Grand Saline SALMON GNOME COWBOY		
20. ABSTRACT (Continue on reverse side if necessary and identify by block number) Finite difference calculations are used to predict the ground motion and RVP spectra from a tamped 200 pound charge of Pelletol explosive detonated in the Grand Saline Salt Dome. Computational constitutive models and material properties for dome salt are first normalized using ground motion data from a number of nuclear and high explosive events in salt including SALMON, GNOME, and COWBOY. The ground motion predictions for Phase III of the Grand Saline experiment are then made using our best guesses for site material properties. (continued)		

DD FORM 1 JAN 73 1473

EDITION OF 1 NOV 65 IS OBSOLETE

Unclassified

SECURITY CLASSIFICATION OF THIS PAGE (When Data Entered)

Unclassified

SECURITY CLASSIFICATION OF THIS PAGE(When Data Entered)

20. Abstract (continued)

We predict an "elastic" radius between 17 to 23 meters and a final cavity radius of approximately 52 centimeters.

Unclassified

SECURITY CLASSIFICATION OF THIS PAGE(When Data Entered)

AFTAC Project Authorization No. VT/0712/B/PMP
ARPA Order No. 2551, Program Code No. 6H189
Effective Date of Contract: November 17, 1978
Contract Expiration Date: November 15, 1981
Amount of Contract: \$1,816,437
Contract No. F08606-79-C-0008
Principal Investigator and Phone No.
Dr. J. Theodore Cherry, (714) 453-0060
Project Scientist and Phone No.
Mr. Brian W. Barker, (202) 325-7581

This research was supported by the Advanced Research Projects Agency of the Department of Defense and was monitored by AFTAC/VSC, Patrick Air Force Base, Florida 32925, Under Contract No. F08606-79-C-0008.

The views and conclusions contained in this document are those of the authors and should not be interpreted as necessarily representing the official policies, either expressed or implied, of the Advanced Research Projects Agency, the Air Force Technical Applications Center, or the U. S. Government.

W/O 11098



A

TABLE OF CONTENTS

<u>Section</u>	<u>Page</u>
I. INTRODUCTION.	1
II. THE CONSTITUTIVE MODEL FOR THE DOME TEST.	2
III. PREDICTIONS FOR THE GRAND SALINE EXPERIMENTS.23
IV. REFERENCES.34
APPENDIX35

LIST OF ILLUSTRATIONS

<u>Figure</u>	<u>Page</u>
1. Strength data for salt obtained from laboratory triaxial compressions tests	3
2. Comparison between SALMON gauge 1E14-20 AR at a range of 274 m and calculated velocity.	5
3. Comparison between SALMON velocity gauge E6-27URH at 318 m and calculated velocity.	6
4. Comparison between SALMON velocity gauge E14C-39 at 402 m and calculated velocity.	7
5. Comparison between SALMON velocity gauge E11-27URH at 620 m and calculated velocity.	8
6. Comparison between SALMON velocity gauge E11-34URB at 658 m and calculated velocity.	9
7. Comparison between SALMON velocity gauge E5-27URH at 742 m and calculated velocity.	10
8. Comparison between calculated and observed peak velocity and displacements for SALMON.	13
9. Calculated RVP spectra at ranges both inside and outside the "elastic" radius of 967 m	14
10. Comparison of calculated and observed RVP spectra for SALMON.	15
11. Comparison of calculated and observed peak velocities for the GNOME event	17
12. Comparison of calculated and observed peak displacements for the GNOME event	18
13. Comparison between calculated and measured velocities at a range of 229 m for the GNOME event	19
14. Comparison between calculated and measured velocities at a range of 298 m for the GNOME event	20
15. Comparison of calculated and observed RVP spectra for GNOME	21
16. Calculated peak velocities versus range for 1 Kg of Pelletol using SALMON material properties	24
17. Calculated peak velocities versus range for 1 Kg of Pelletol using COWBOY material properties	25
18. Calculated peak displacements versus range for 1 Kg of Pelletol using SALMON material properties.	26
19. Calculated peak displacements versus range for 1 Kg of Pelletol using COWBOY material properties.	27

LIST OF ILLUSTRATIONS (Continued)

<u>Figure</u>		<u>Page</u>
20.	Computed RVP spectra at the elastic radii using SALMON material properties and COWBOY properties for a yield of 200 pounds of Pelletol31
21.	Calculated RVP spectra of Figure 20 simply scaled to SALMON yield compared to RVP spectra for gauge 2.4 - 15-V from COWBOY 11 scaled to 5.3 KT by Trulio using HE-nuclear equivalence relation32

I. INTRODUCTION

A series of high explosive tests is presently being conducted for DARPA in the Grand Saline Salt Dome near Dallas, Texas. Phase I of the experimental program consisted of passive measurements from 25 gm explosive charges detonated in the Hockley Salt Mine near Houston, Texas. Phase II of the program involved passive measurements from 200 pound charges of nitromethane and powdered TNT (Pelletol), is near completion. In Phase III of the experimental program, one-tamped 200 pound charge of Pelletol will be detonated in the summer of 1982 and ground motion measurements made to determine the extent of inelastic effects on velocity and displacement pulses down to peak radial velocity of approximately 1 cm/sec.

In this report, we predict the ground motion from Phase II of the Grand Saline experiment using computational constitutive models and material properties for dome salt which have been normalized to ground motion data from a number of nuclear and high explosive events in salt. These events include GNOME, SALMON, STERLING, and COWBOY (see Cherry and Rimer, 1980). The ground motion predictions are made using our best guesses for site material properties (wave speeds, strength, etc.) in the absence of laboratory or in situ properties data from the Grand Saline site.

In Section II of this report, we discuss the normalization of the constitutive models to the SALMON 5.3 KT nuclear event and indicate the changes in material properties required to simulate the COWBOY tamped high explosive (Pelletol) tests. Our predictions for the ground motion for Phase III of the Grand Saline experiment are discussed in Section III. Plots of calculated velocities versus time at 14 ranges from the explosive are given in the Appendix.

II. THE CONSTITUTIVE MODEL FOR THE DOME TEST

The 5.3 KT SALMON nuclear event in the Tatum Salt Dome in Mississippi provides a large subset of the available free-field near source, ground motion data in the form of digitized records of particle velocity versus time which are extremely consistent with range from the working point. For this reason, the SALMON event was chosen for the normalization of the constitutive model used in the one-dimensional explosion calculations. The normalized model was then applied to the remaining salt events GNOME, STERLING, and COWBOY as described by Cherry and Rimer (1980) to show that a single constitutive model could explain much of the salt ground motion data. Here we detail the salt constitutive model and show some results of the normalization.

Figure 1 shows the laboratory strength data for SALMON, GNOME, and Polycrystalline salt. The curve shown in the figure fits the data for SALMON and GNOME and was used in the model for the ultimate strength of salt (Y_{Lim}).

The best agreement with the SALMON ground motion data was obtained by assuming that salt work hardened to its ultimate strength. The expression used to calculate the strength (Y) as a function of the inelastic energy (E) deposited in the material during yielding was:

$$Y = Y_0 (1 + e_1 E - e_2 E^2) \leq Y_{Lim}$$

where Y_0 is the initial strength and e_1 and e_2 are respectively work hardening and work softening material constants.

If S_{ij} is the deviatoric component of the stress tensor and J_2 is the unadjusted second deviatoric invariant, then the increment in inelastic energy becomes

$$\Delta E = S_{ij} \Delta \epsilon_{ij} = \frac{S_{ij} S_{ji}}{2\mu} \frac{\sqrt{3J_2} - Y}{Y}$$

where

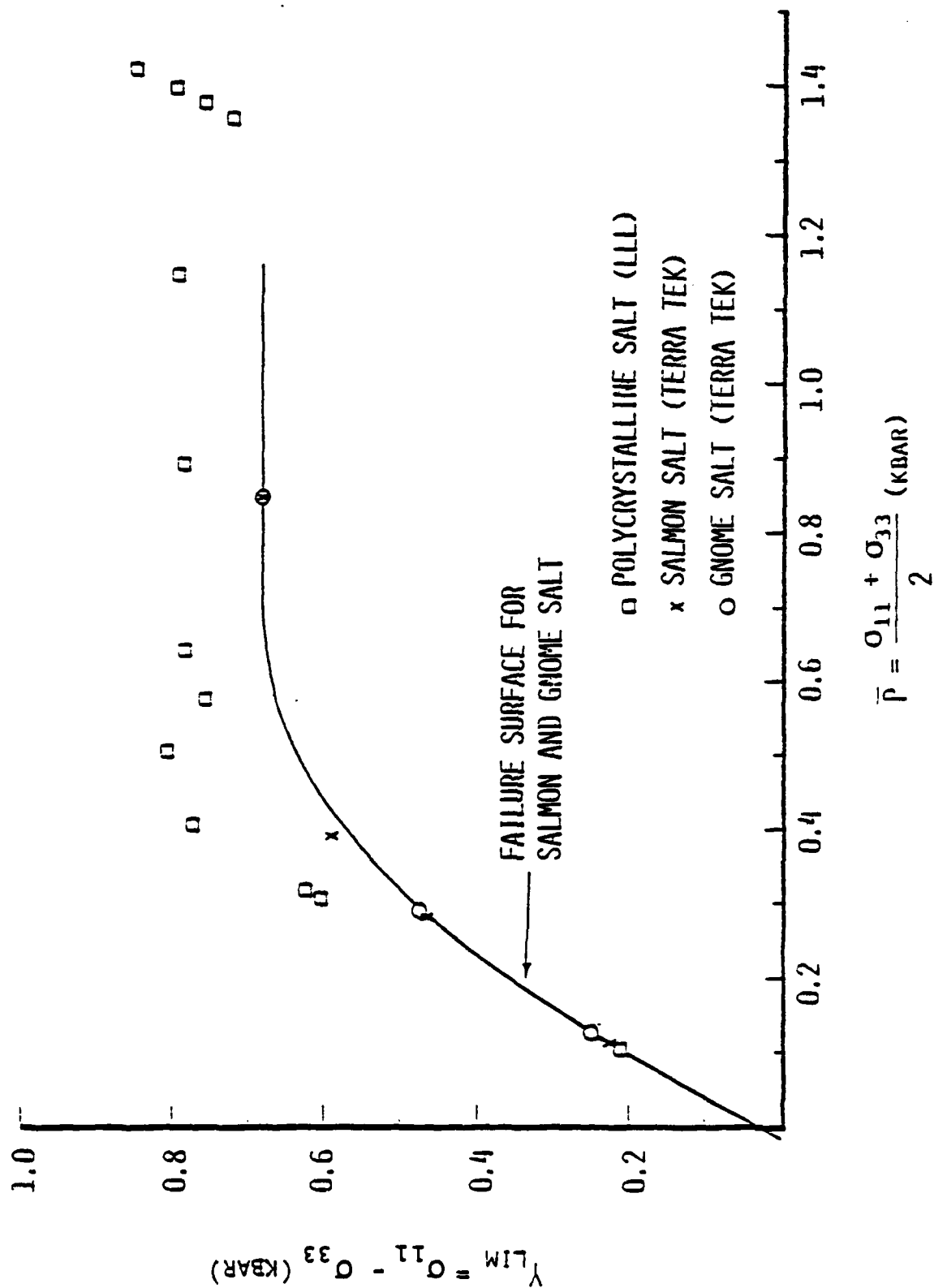


Figure 1. Strength data for salt obtained from laboratory triaxial compression tests.

$$3J_2^i > \gamma^2$$

π_{ij} = the deviatoric component of the inelastic strain tensor

μ = the shear modulus .

This model is simple and easily implemented in a finite difference stress wave code. Figures 2 through 7 show the agreement between the SALMON particle velocity data (the solid curves) and the calculations (the dotted curves) made with this model and the normalizing material constants given in Table 1.

The work hardening aspect of the model was required in order to explain a number of puzzling features of the particle velocity data, the most important being a small amplitude "elastic" precursor which is not consistent with the laboratory strength measurements of Figure 1 or with the overburden pressure at shot depth. In the data of Figures 2 through 7, the "elastic" precursors have peak velocities of approximately 0.3 - 0.4 m/sec, consistent with a strength of approximately 25 bars. However, such a low strength at a mean stress larger than the overburden pressure of approximately 175 bars would imply a velocity pulse width at least a factor of two broader than the data.

This conflict between the low material strengths associated with the precursor and the much higher strengths required to narrow the pulse following the precursor can be resolved if salt is assumed to work harden after the strength γ_0 of 25 bars is attained. However, the strength of 25 bars is still much lower than would be anticipated at the overburden pressure (see Figure 1). We concluded that the rock does not feel the overburden, i.e., that the effective stress is zero and γ_0 is the saturated strength of the rock. The physical explanation for the work hardening during loading may be an increase in the effective stress and, conversely, a decrease in pore fluid pressure caused by dilatancy.

It is interesting that salt apparently requires a constitutive model different from those used for the rocks at NTS. They all have

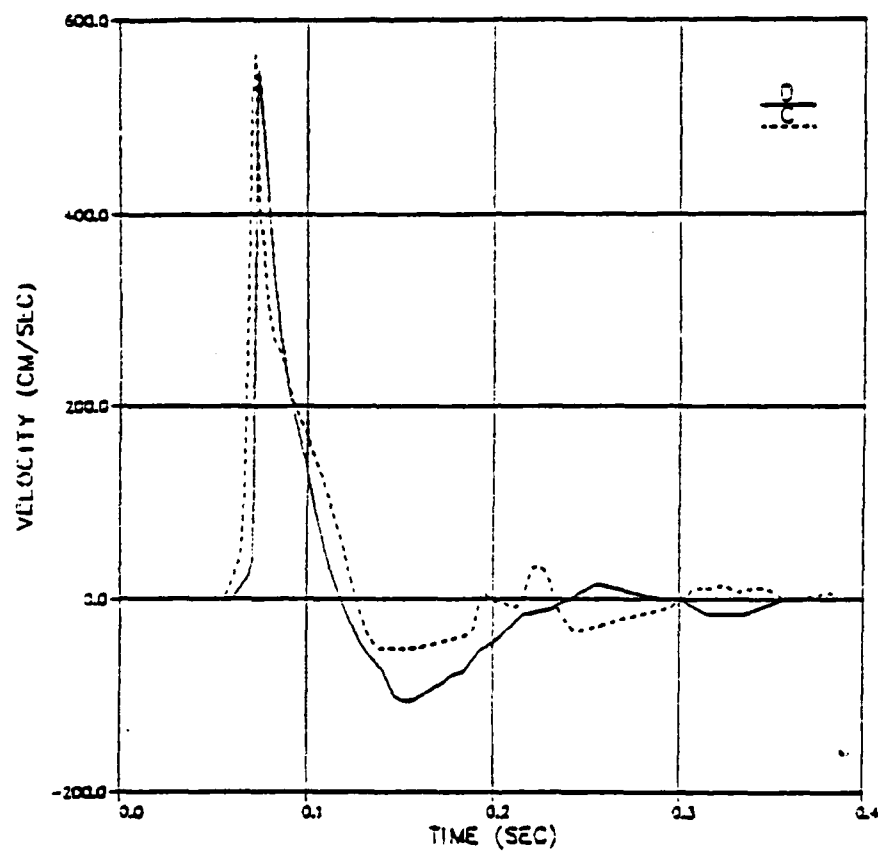


Figure 2. Comparison between SALMON gauge 1E14-20 AR at a range of 274 m and calculated velocity (the dotted curve).

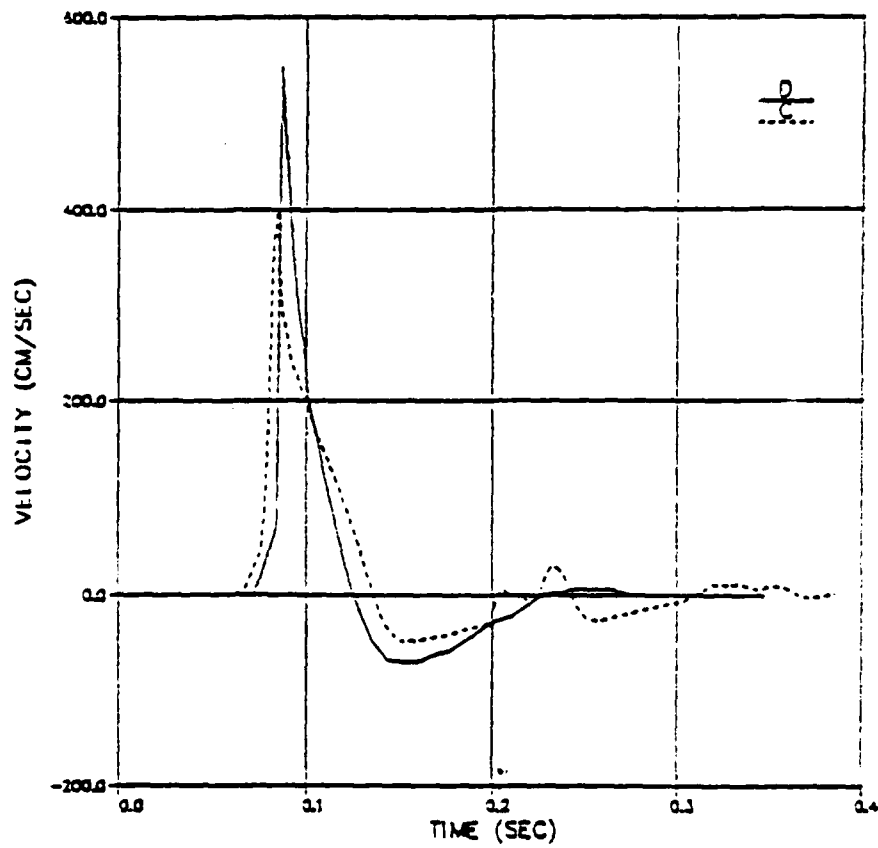


Figure 3. Comparison between SALMON velocity gauge E6-27URH at 318 m and calculated velocity.

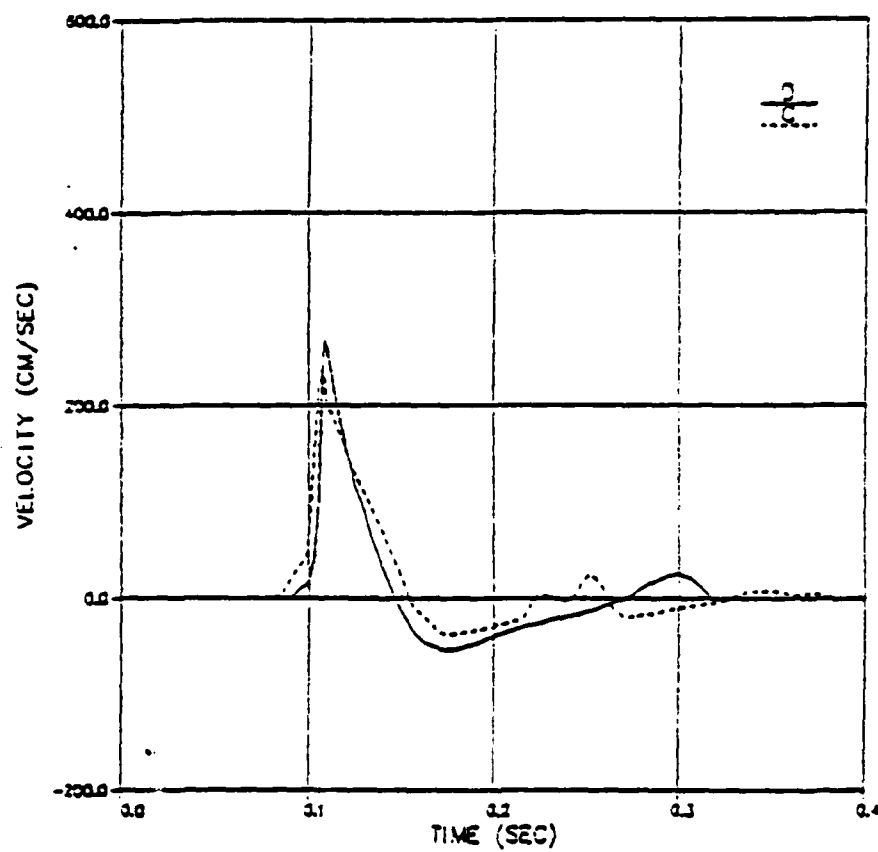


Figure 4. Comparison between SALMON velocity gauge E14C-39 at 402 m and calculated velocity.

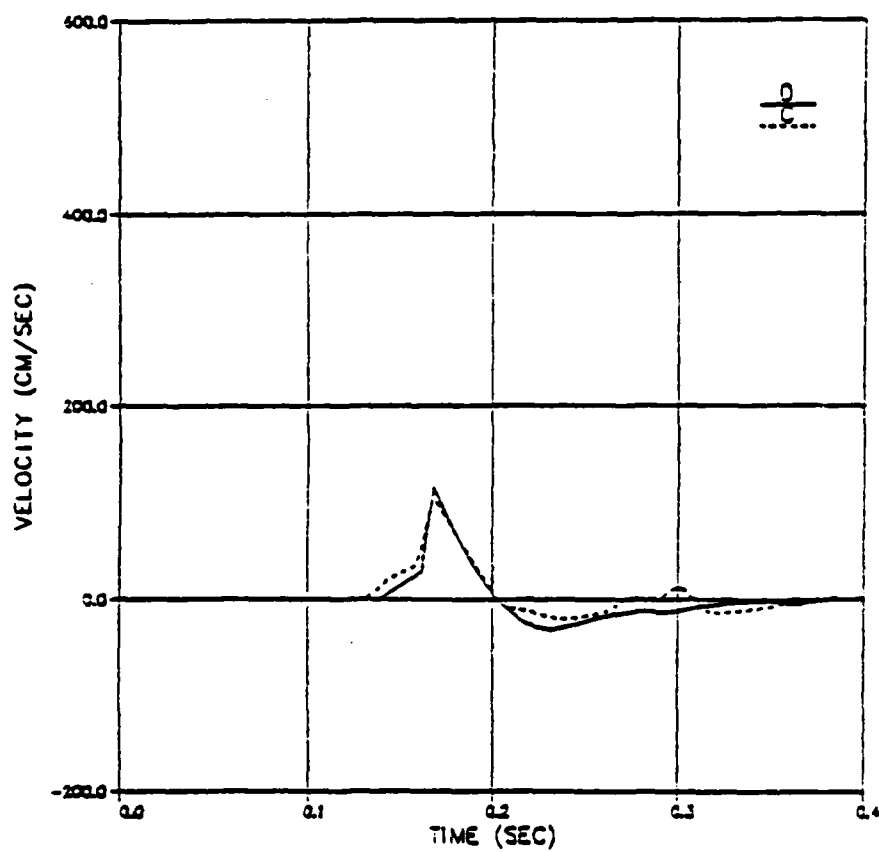


Figure 5. Comparison between SALMON velocity gauge E11-27URH at 620 m and calculated velocity.

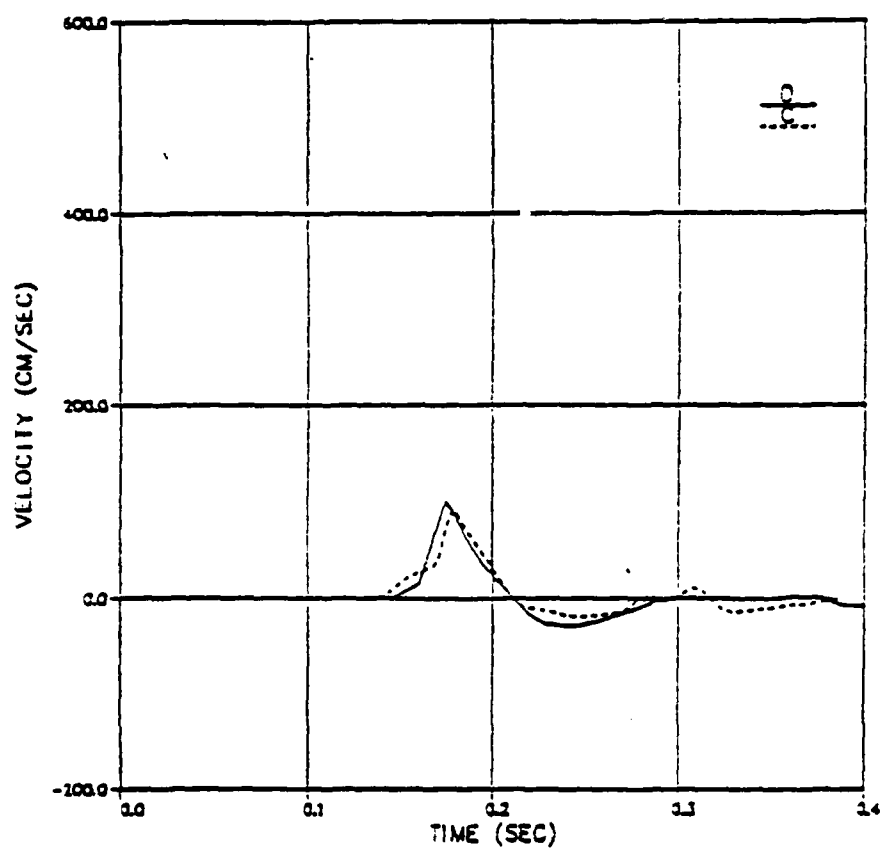


Figure 6. Comparison between SALMON velocity gauge E11-34URB at 658 m and calculated velocity.

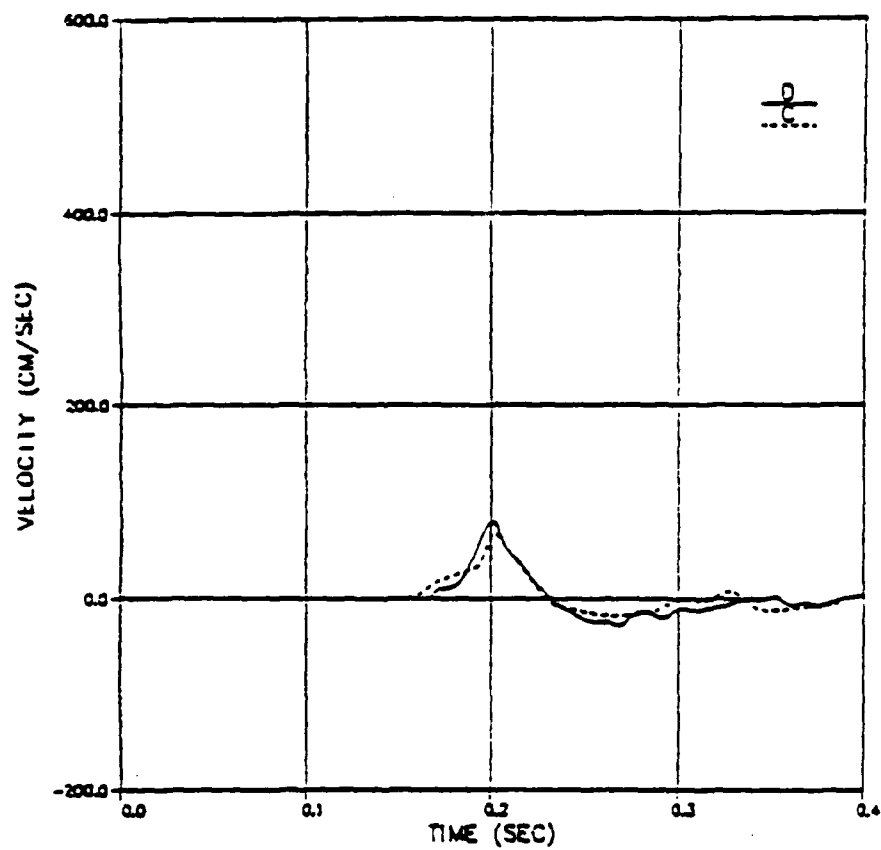


Figure 7. Comparison between SALMON velocity gauge E5-27IURH at 742 m and calculated velocity.

Table 1

MATERIAL PROPERTIES FOR DOME SALT

Property	SALMON	GNOME	COWBOY
P-wave velocity (m/sec)	4,550	4,317	4,375
S-wave velocity (m/sec)	2,540	2,306	2,550
Density (gm/cc)	2.2	2.2	2.2
Y_0 (Kbar)	0.025	0.025	0.04
Y_{Lim} (Kbar)	0.680	0.680	0.70
Hardening e_1 ($\frac{cc}{erg}$)	6.E-5	6.E-5	6.E-5
Softening e_2 ($\frac{cc}{erg}$) ²	1.E-12	1.E-12	1.E-12

one feature in common, however, namely that seismic coupling is strongly influenced by low strength states, i.e., those that are between the tensile strength and the unconfined compressive strength. This reduction in strength has been attributed to pore fluid pressure and effective stress. Therefore, the degree of saturation at shot depth and the location of the water table are critical seismic coupling site properties. In addition, it is important that laboratory strength data be obtained for critical rock types at stress states below unconfined compression.

The work hardening constants of the constitutive model for salt were normalized to give best agreement with the measurements from SALMON shown in Figures 2 through 7. Figure 8 compares the calculated and observed peak velocities and peak displacements (the stations of Figures 2 through 7 are identified in the figure by an "X"). The results of two calculations are shown in this figure: one (dashed curve) in which Y_{Lim} equaled the maximum strength (0.68 Kb) given in Figure 1, and the second (solid curve) in which Y_{Lim} varied with stress state (\bar{P}) as shown in Figure 1.

Shear failure was calculated out to a range of 967 m. Beyond this "elastic" radius, the peak velocity in the calculation is determined by the precursor. Note that this "elastic" radius is larger than all ranges of the SALMON data shown in Figure 8. Figure 9 shows the RVP spectra ($|\hat{\psi}|$) for the two calculations at the ranges of Figures 2 through 7 and beyond the calculated elastic radius where the spectra are invariant with range. Figure 10 shows the spectra from beyond the elastic radius for the two calculations together with the spectra of Springer, et al. (1968), which represents an average of the free field SALMON data, and Murphy, which was obtained by scaling the spectrum of the GNOME event to the yield and depth of SALMON.

These results, involving comparisons between calculated and observed ground motions and RVP spectra indicate that the constitutive model adequately explains the SALMON data. The constitutive model was then applied to the simulation of the 3.1 KT GNOME event which was detonated in a salt medium near Carlsbad, New Mexico. The calculation used the work hardening constants

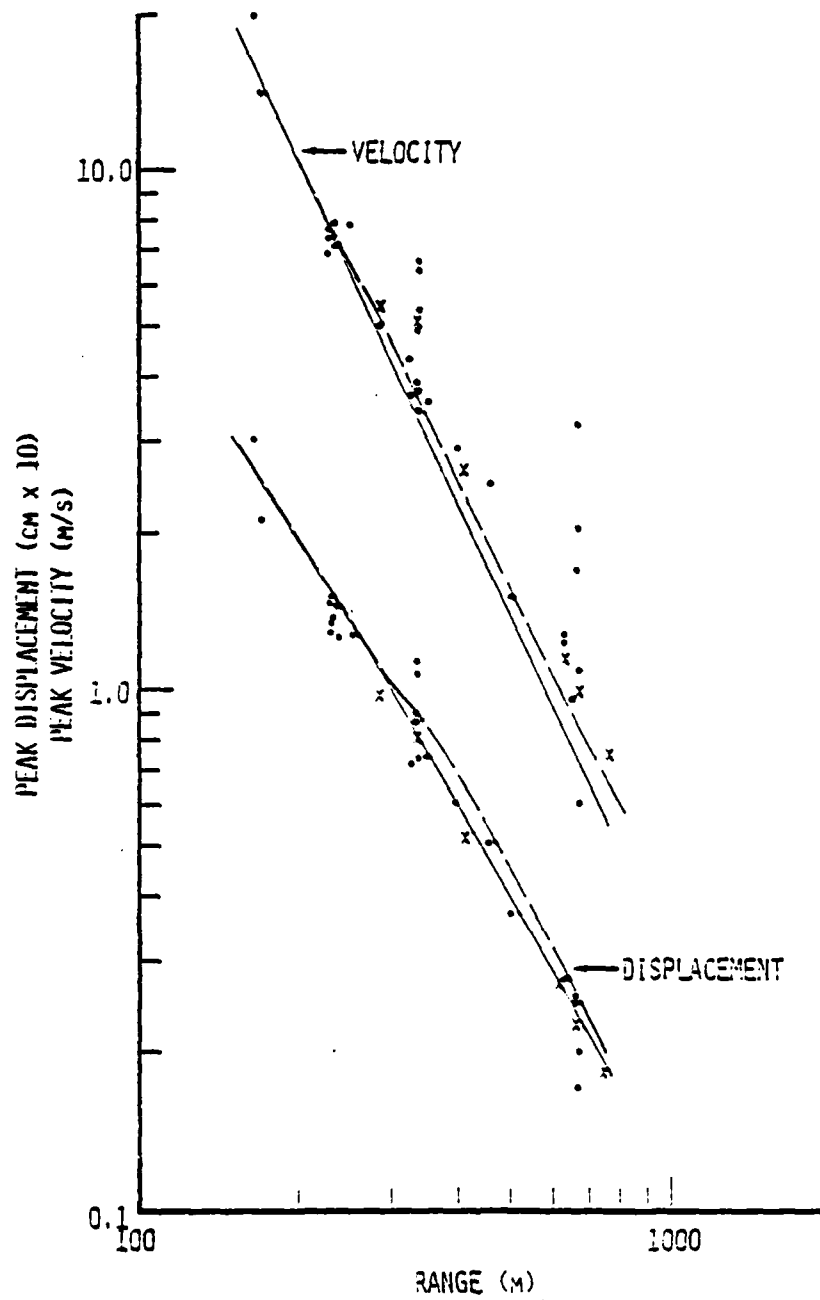


Figure 8. Comparison between calculated and observed peak velocity and displacements for SALMON.

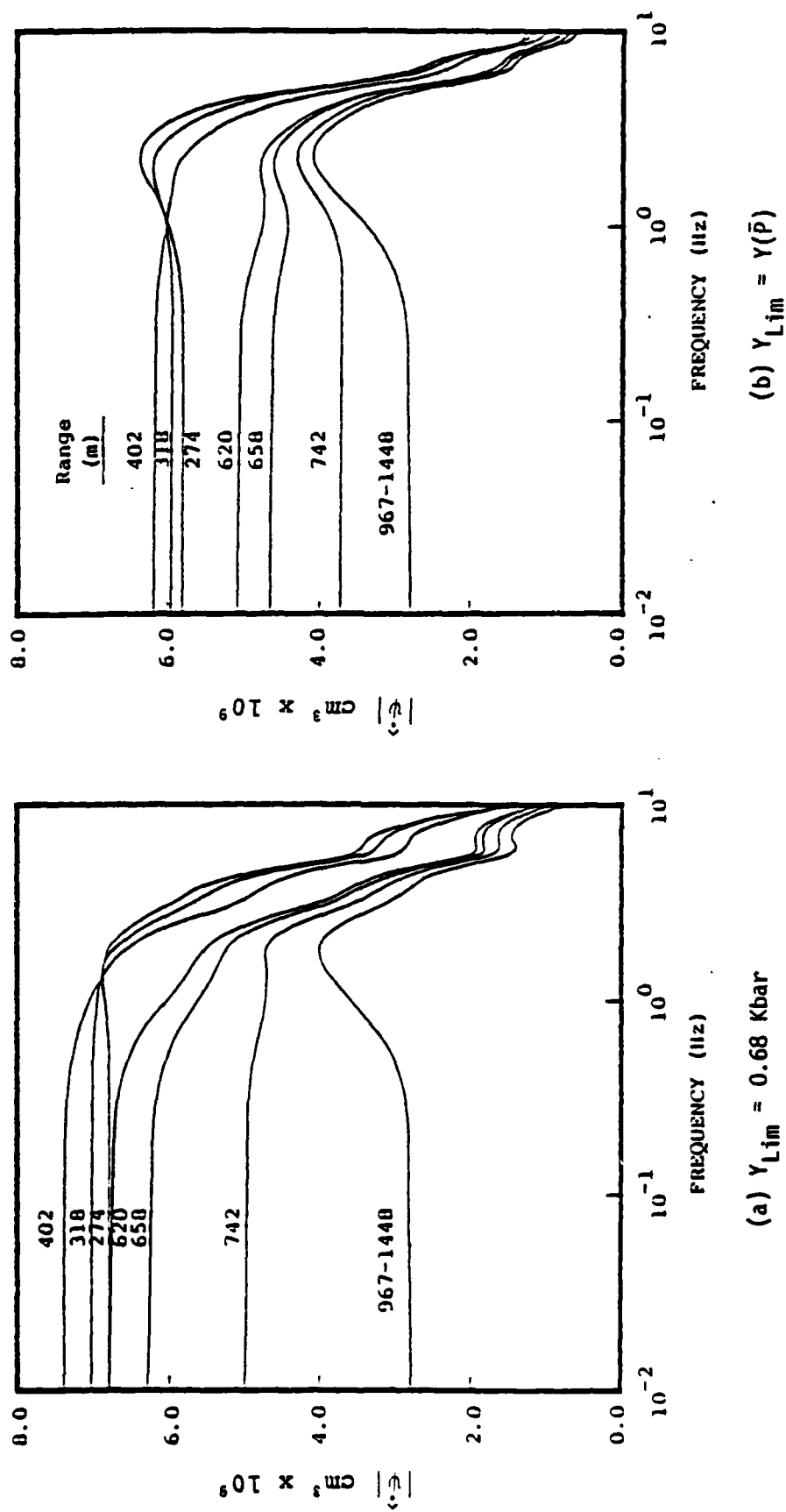


Figure 9. Calculated RVP spectra ($|\hat{\psi}|$) at ranges both inside and outside the "elastic" radius of 967 m.

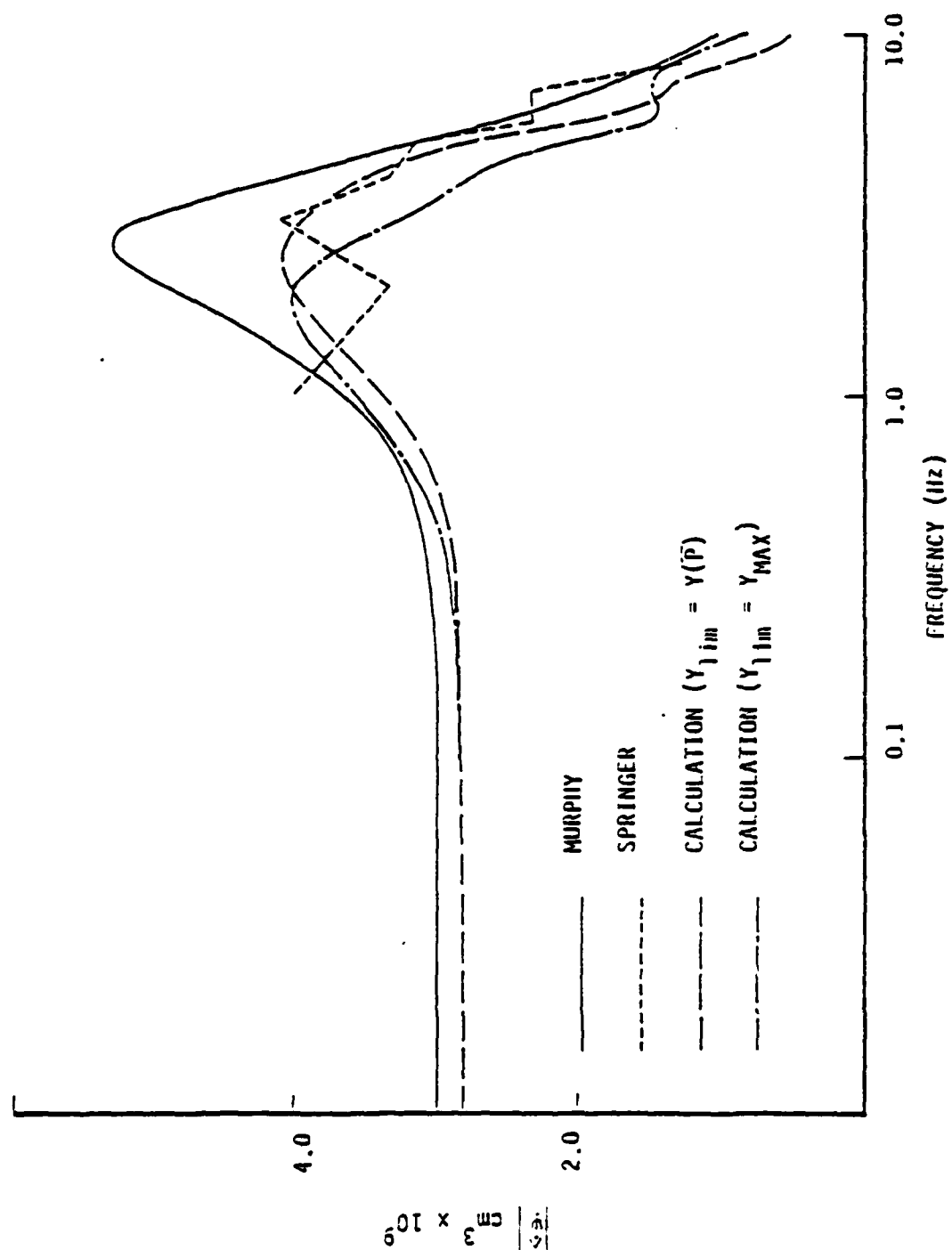


Figure 10. Comparison of calculated and observed RVP spectra for SALMON.

normalized for SALMON, the wave speeds measured for GNOME (see Table 1), and the GNOME overburden pressure of 80 bars, and gave a calculated cavity volume within 9 percent of the measurement.

Figures 11 and 12 compare calculated and observed peak velocities and peak displacements for this event. Figures 13 and 14 compare calculated and measured velocities at ranges of 229 and 298 m respectively. All show a precursor similar to that observed for SALMON. The calculated elastic radius for the GNOME event was 790 m.

Figure 15 compares the Mueller-Murphy estimate of the GNOME RVP spectrum with the calculated spectrum. Agreement is surprisingly good considering that the Mueller-Murphy spectrum was based on ground motion data at a range of 300 m, a distance well within the region of nonlinear material behavior.

The constitutive model was next applied to the COWBOY tamped, high explosive events in the Winnfield Salt Dome in Louisiana. The high explosive, Pelletol, consisting of small pellets of TNT of density 1 gm/cc, has not been well-characterized in the dry state used for the COWBOY tests. Upon the recommendation of E. Lee of Lawrence Livermore Laboratory, we used the JWL equation of state constants for HNS powder (Lee, et al., 1976) which very closely resembles TNT in composition and molecular structure, to characterize Pelletol.

Calculations were made for COWBOY with these HE properties both using the SALMON material properties and using the wave speeds and strength modifications appropriate to COWBOY as given in Table 1. Both calculations gave good agreement with the measured peak velocities. Calculated peak displacements were a factor of two higher than the measurements when SALMON material properties were used and approximately 50 percent higher than the measurements when COWBOY properties were used in the calculations.

Trulio (1978) recommended two modifications of the JWL constants for HNS to better characterize the Pelletol explosive. These were a reduction in the energy yield of the explosive from

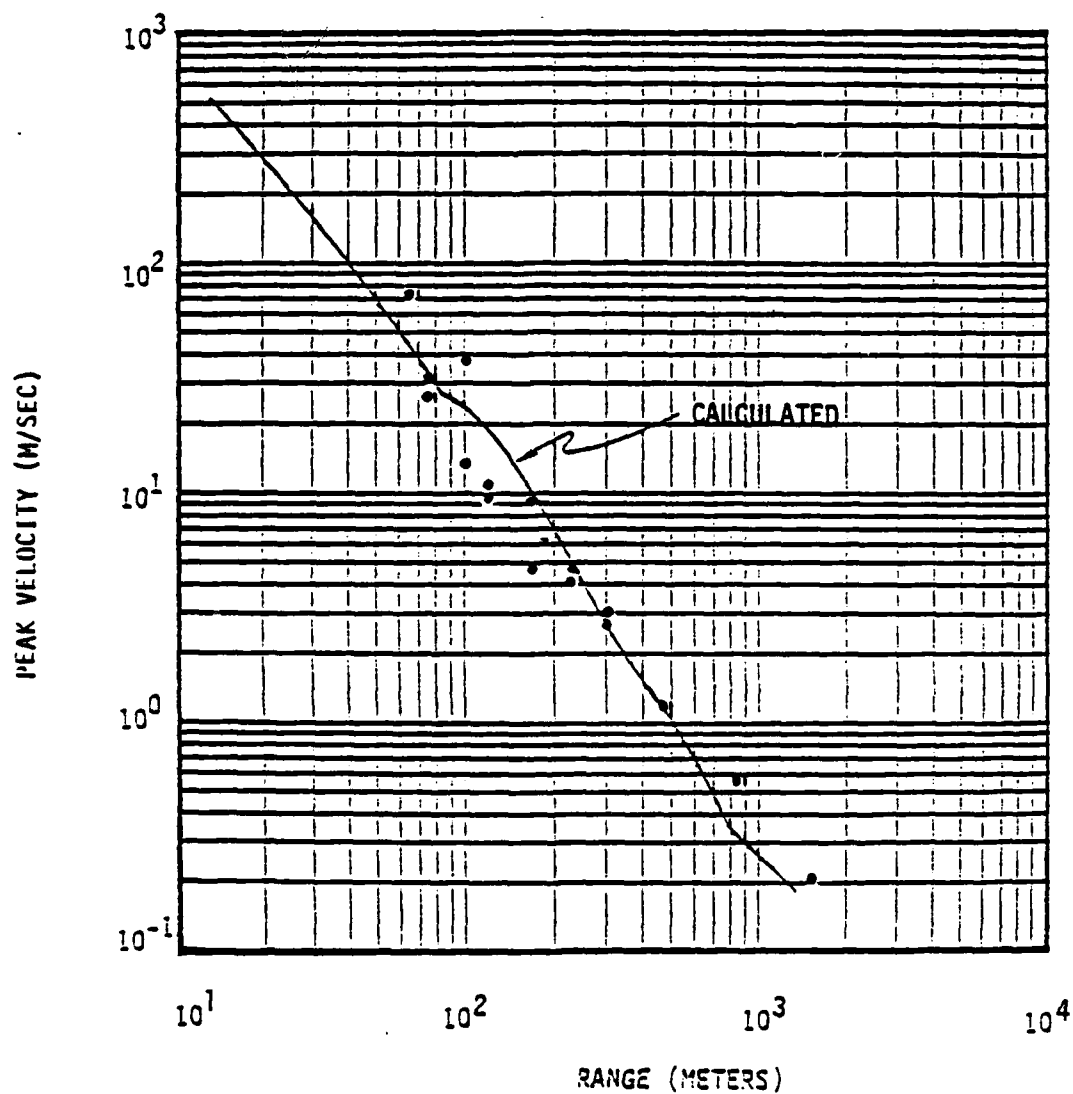


Figure 11. Comparison of calculated and observed peak velocities for the GNOME event.

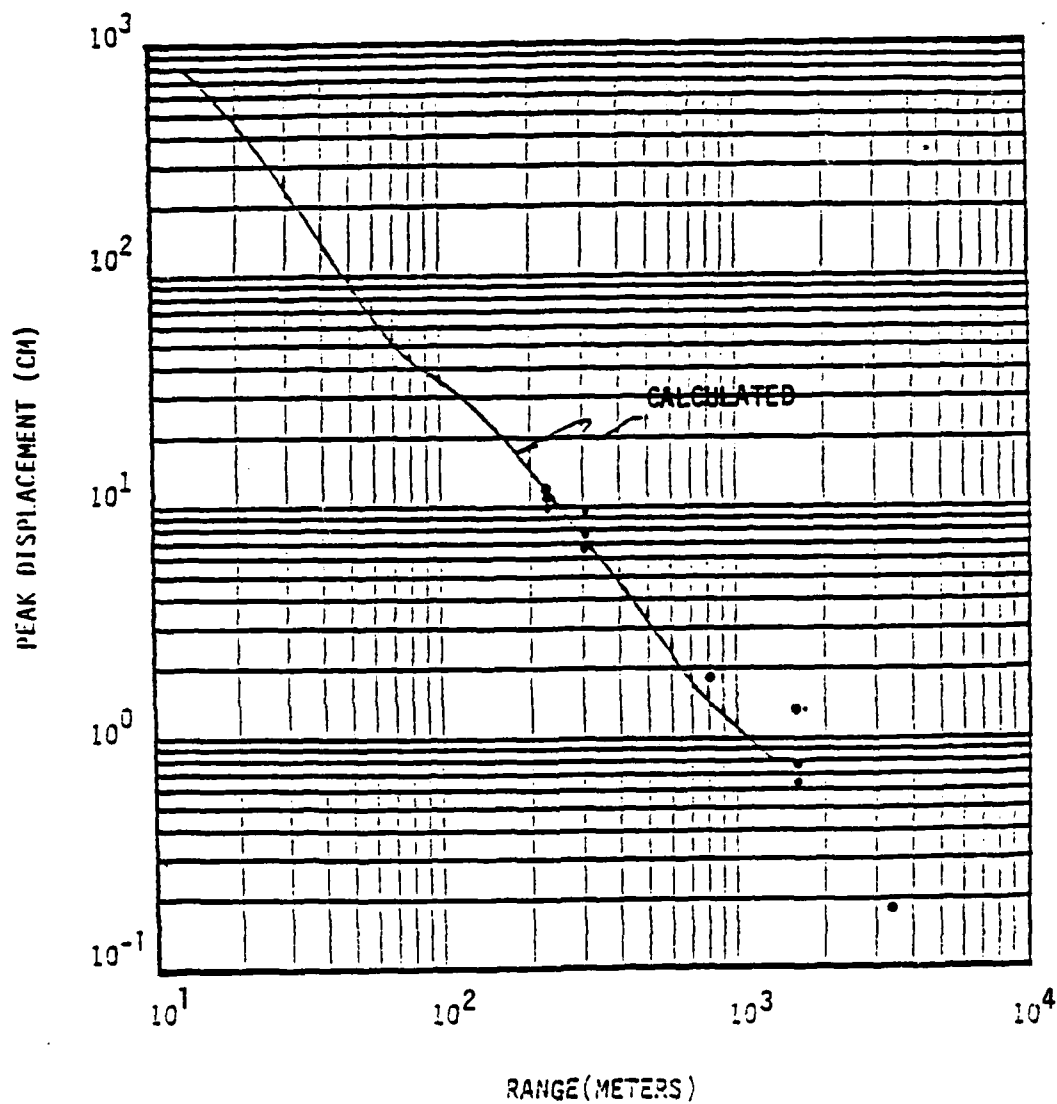


Figure 12. Comparison of calculated and observed peak displacements for the GNOME event.

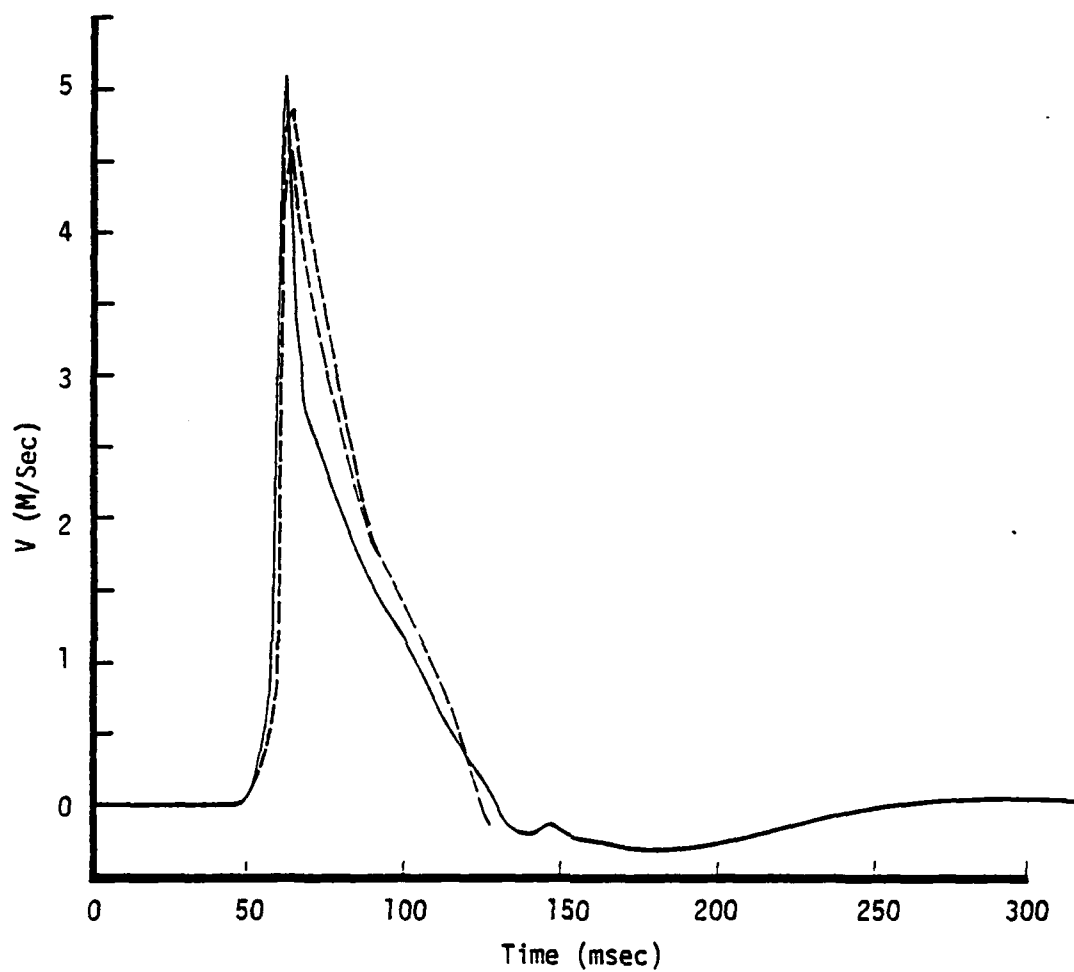


Figure 13. Comparison between calculated (solid curve) and measured velocities at a range of 229 m for the GNOME event.

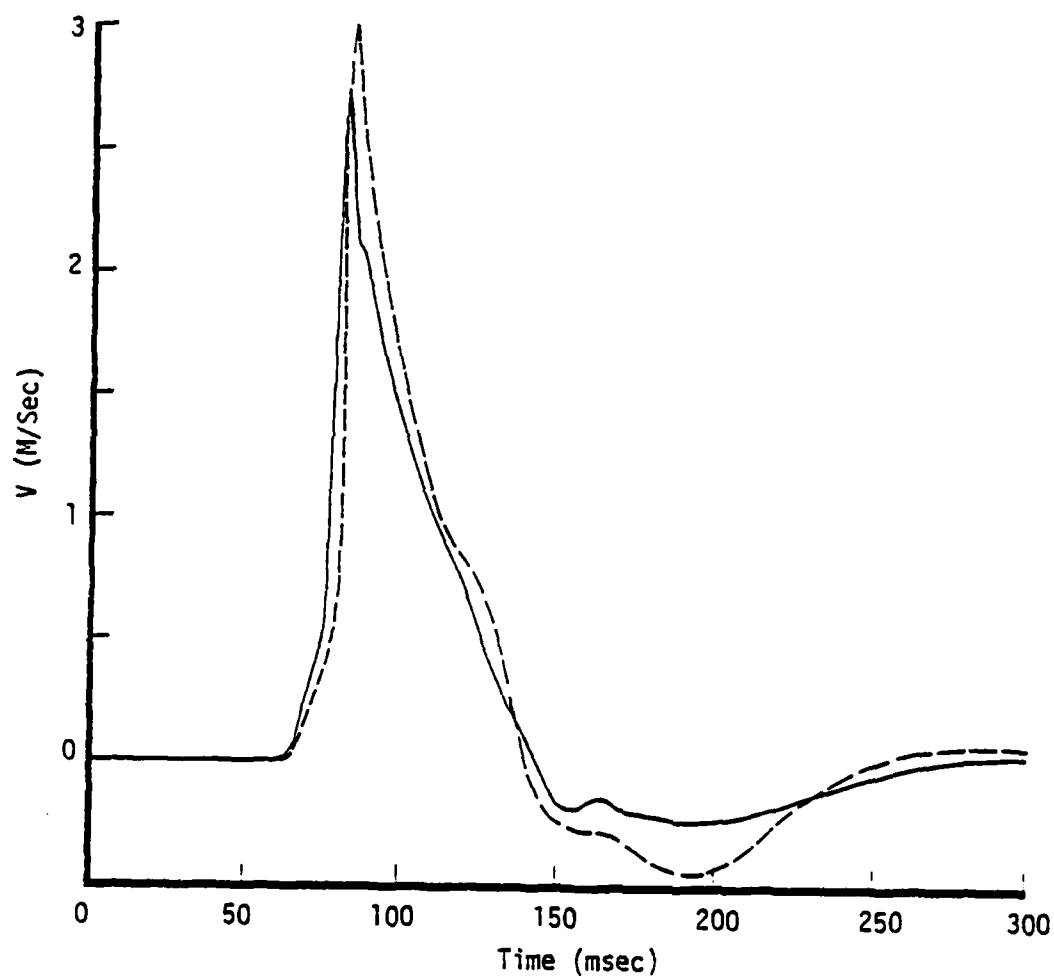


Figure 14. Comparison between calculated (solid curve) and measured velocities at a range of 298 m for the GNOME event.

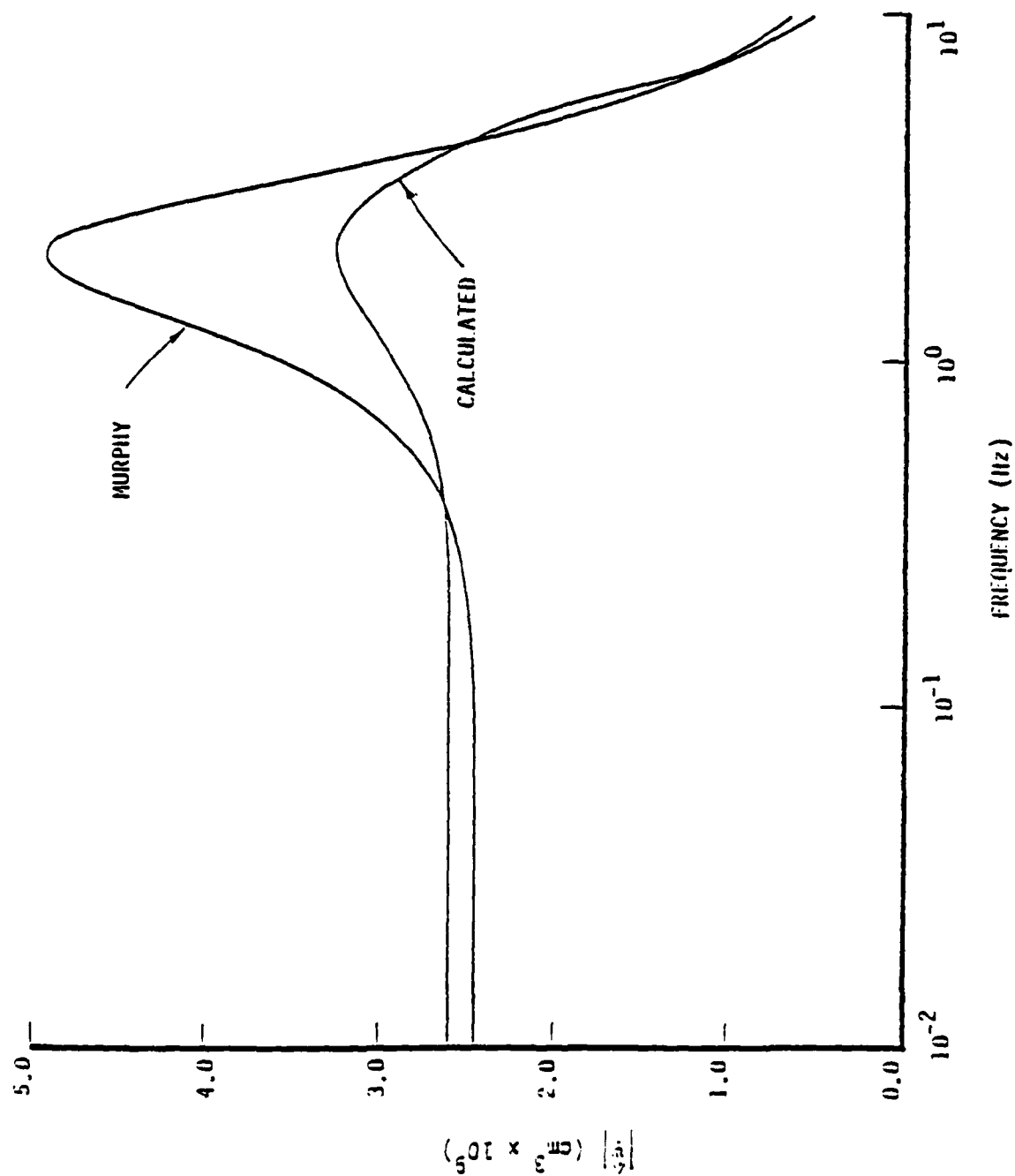


Figure 15. Comparison of calculated and observed RVP spectra for GNOME.

4.1×10^{10} ergs/gm to 2.55×10^{10} ergs/gm and a reduction in w from 0.25 to 0.23 (w is the value of $\gamma-1$ in the ideal gas equation of state of the expanded HE products). Calculations made with this modified Pelletol equation of state gave good agreement with measured peak velocities and peak displacements. These calculational results were then used to make predictions for the Grand Saline event in the absence of material properties information from the site.

III. PREDICTIONS FOR THE GRAND SALINE EXPERIMENTS

At this time, material properties information about the Grand Saline site (wave speeds, strength measurements, etc.) are not available. For this reason, our predictions for Phase III, a tamped 200 pound Pelletol event at a hydrostatic overburden pressure of approximately 60 bars (similar to COWBOY) will be based on results from two calculations: one using our estimates of SALMON material properties, and the other using the estimates of COWBOY properties, both given in Table 1. In this way, we hope to bound the ground motion from the upcoming experiment. The constitutive models for salt, as discussed in Section II, are the same for both bounding calculations, and both use the modified Pelletol equation of state from Trulio (1978).

Figures 16 and 17 show the calculated peak velocities versus range (scaled to 1 Kg, of Pelletol) using the material properties from SALMON and COWBOY respectively. Measured peak velocities from COWBOY, scaled to 1 Kg, are shown on the plots. Figures 18 and 19 show calculated peak displacements for 1 Kg of Pelletol together with COWBOY data. Calculated "elastic" radii from the two calculations are 5.19 meters and 3.80 meters respectively for 1 Kg of Pelletol (23.3 meters and 17.1 meters respectively at the 200 pound yield of Phase III). Note that most of the scaled COWBOY data lie outside of the calculated elastic or shear failure radii. This was not true for the SALMON and GNOME data shown in Figures 8, 11 and 12.

Beyond the elastic radius, the calculated peak velocities and peak displacements shown in Figures 16 through 19 should vary inversely with range (at a slope of minus 1 in the log-log plots) denoting linear elastic behavior. However, these calculated peak velocities and displacements attenuate at a faster than the elastic rate because of the numerical artificial viscosity employed to stabilize the finite difference calculations.

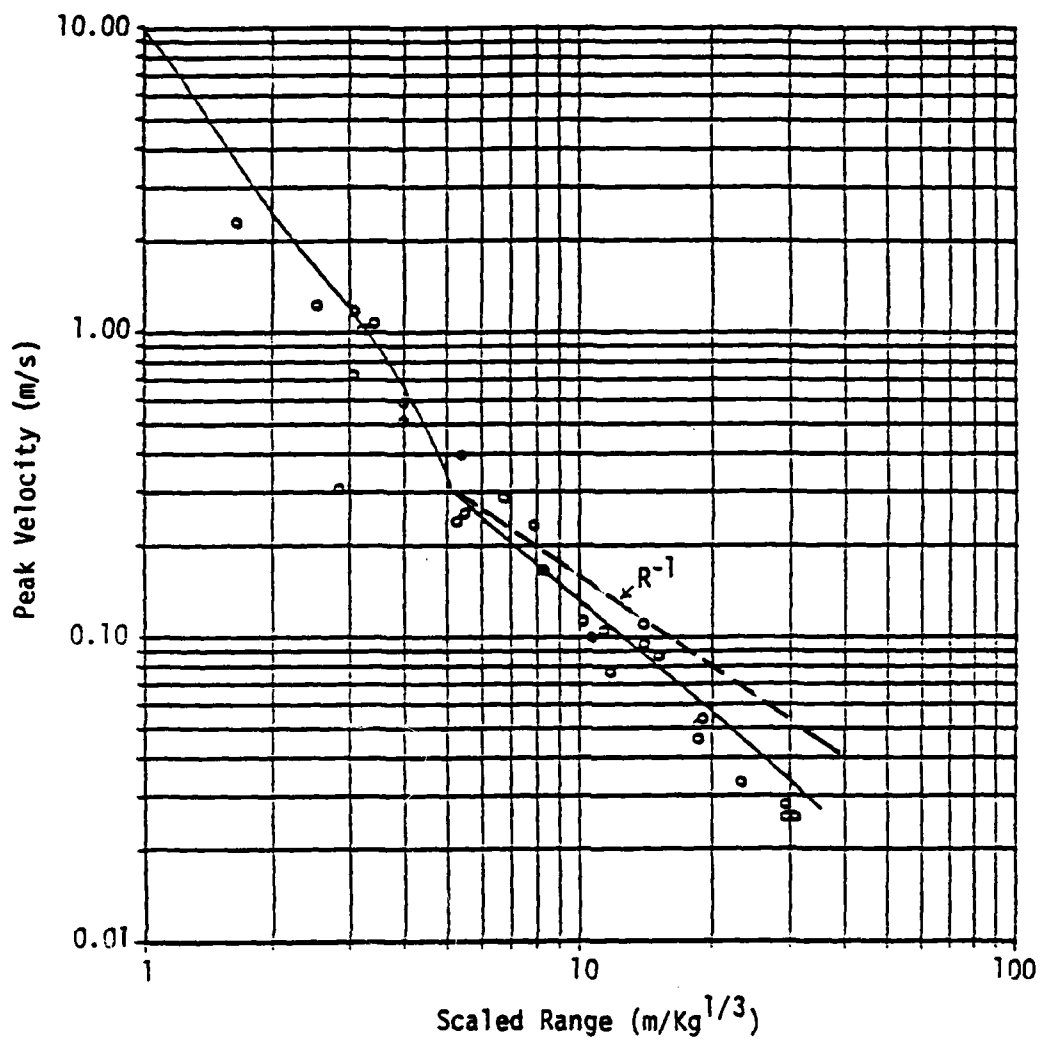


Figure 16. Calculated peak velocities versus range for 1 Kg of Pelletol using SALMON material properties. COWBOY data is shown scaled to 1 Kg.

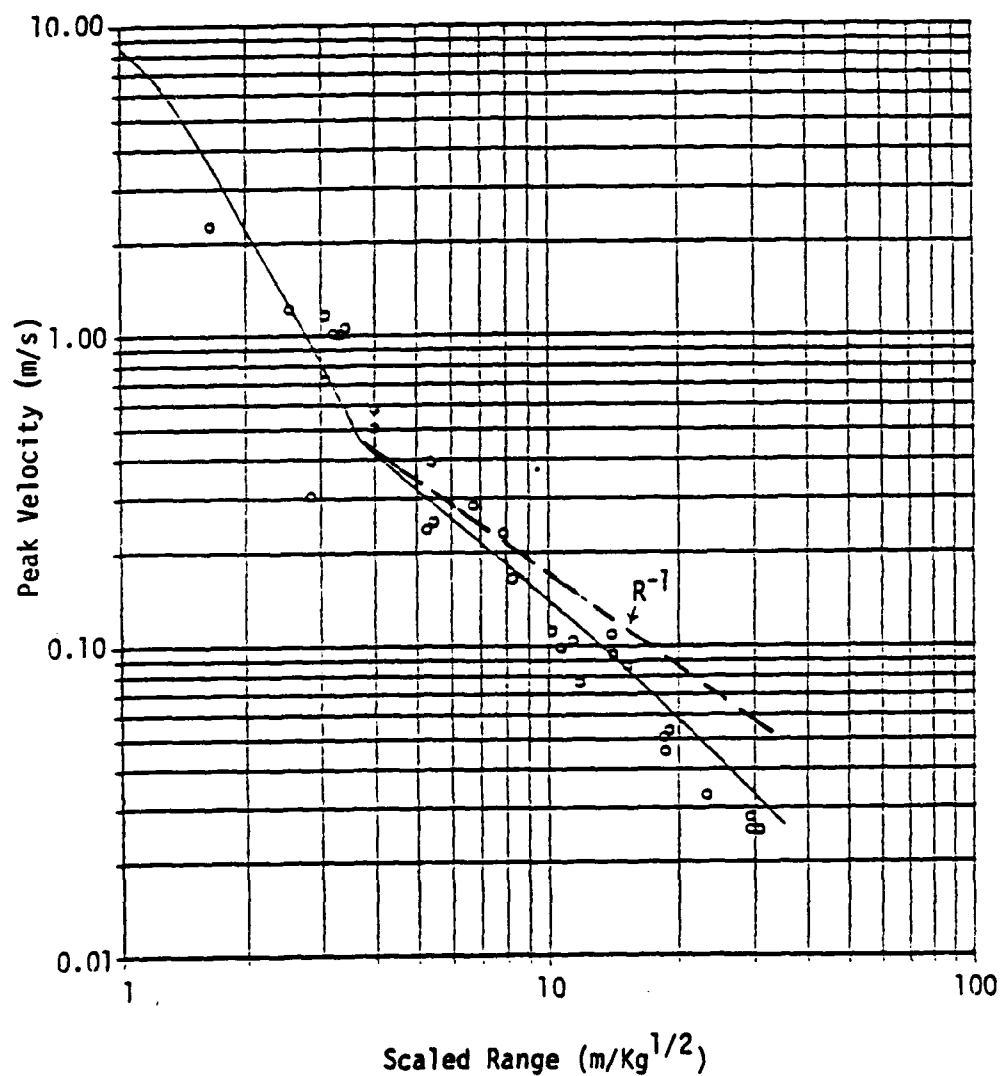


Figure 17. Calculated peak velocities versus range for 1 Kg of Pelletol using COWBOY material properties. COWBOY data is shown scaled to 1 Kg.

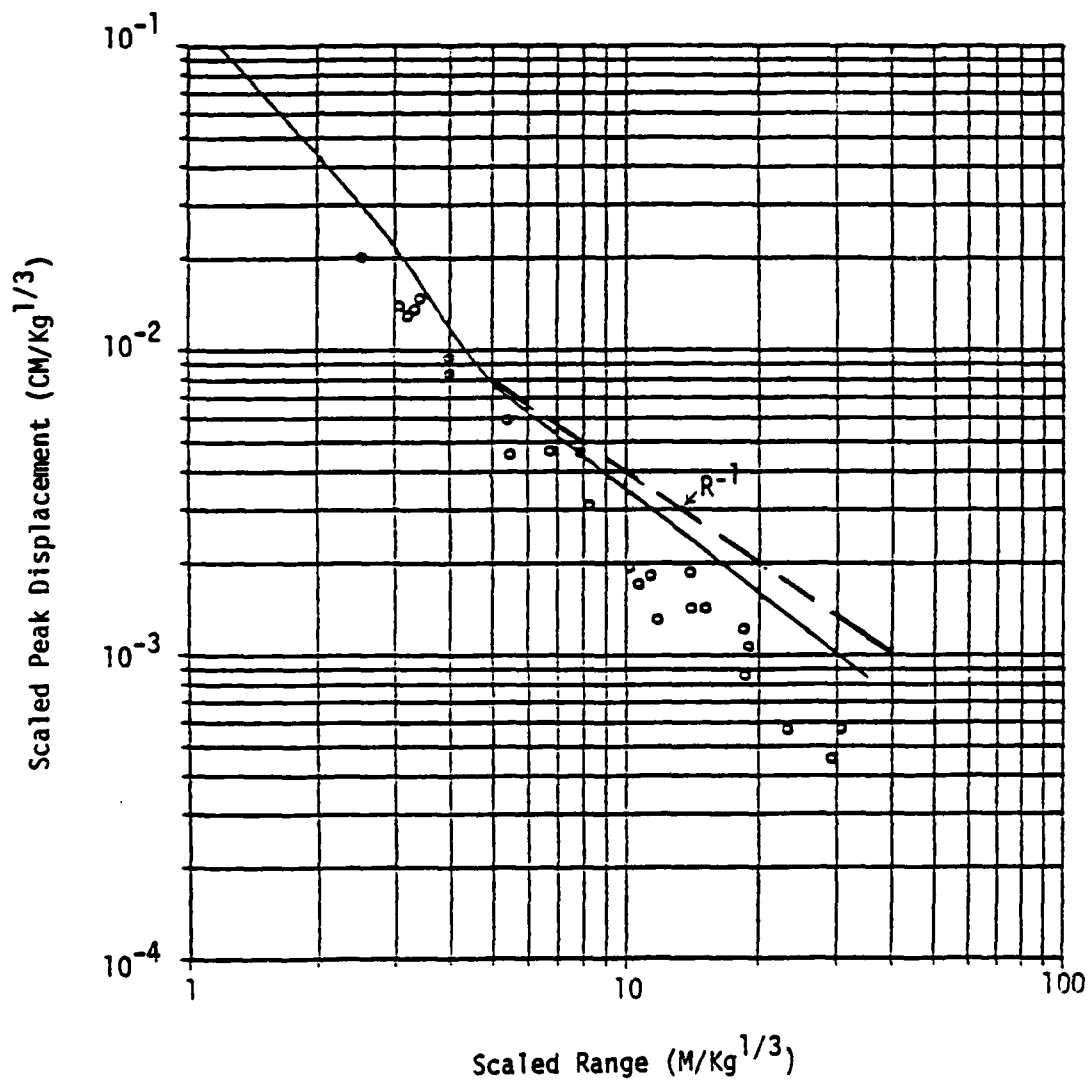


Figure 18. Calculated peak displacements versus range for 1 Kg of Pelletol using SALMON material properties. COWBOY data is shown scaled to 1 Kg.

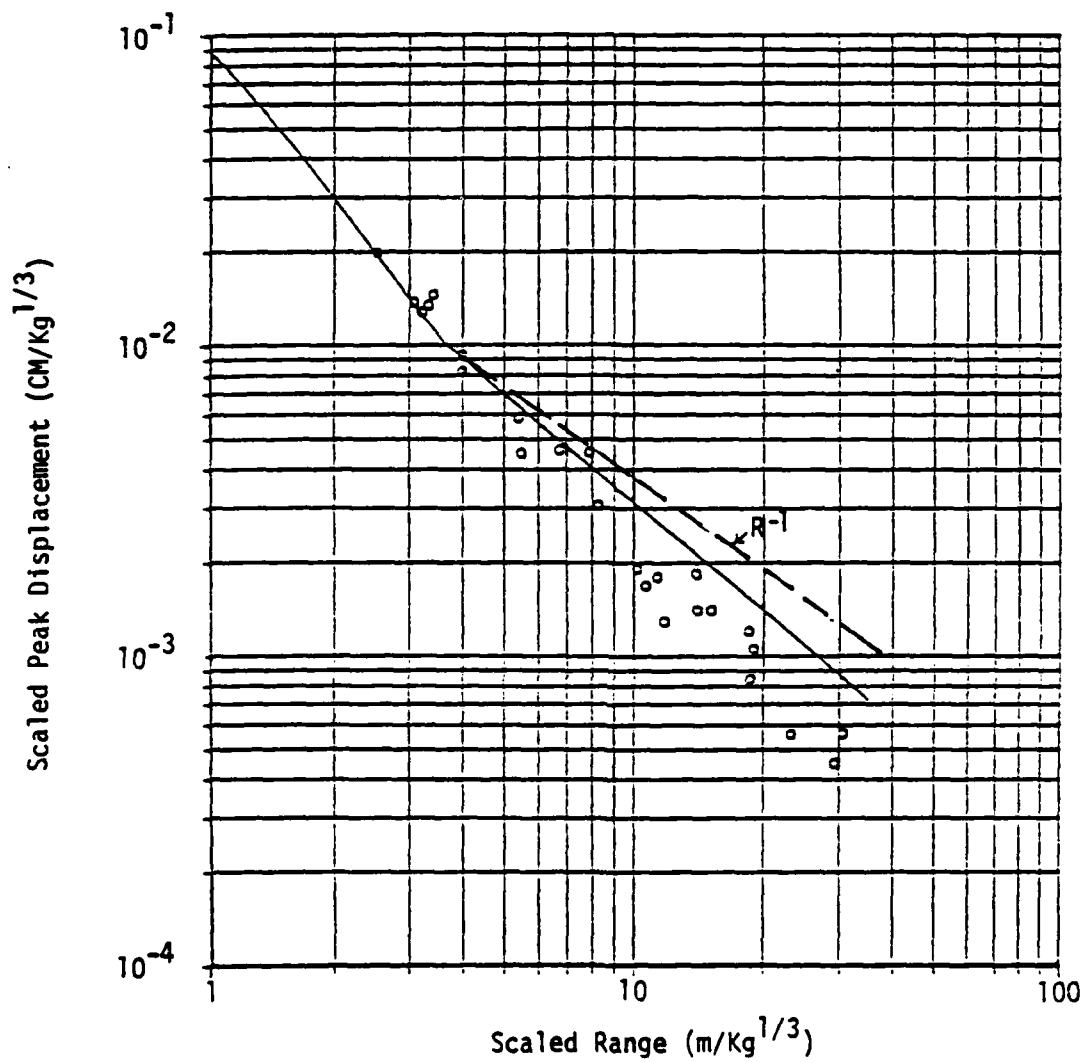


Figure 19. Calculated peak displacements versus range for 1 Kg of Pelletol using COWBOY material properties. COWBOY data is shown scaled to 1 Kg.

The artificial viscosity used in the calculations is a Voigt solid formulation in which the elastic constants k and μ are replaced by the operators $k + k' \frac{\partial}{\partial t}$ and $\mu + \mu' \frac{\partial}{\partial t}$, where

$$k' = c \rho \alpha \Delta r \quad (3.1)$$

$$\mu' = 0 \quad (3.2)$$

and c is a constant, ρ is density, α is P-wave velocity, and Δr is the zone size used in the calculation. This viscosity is artificial, i.e., nonphysical because it depends on the zone size.

Fortunately, the affect of this type of viscoelasticity can easily be removed from the wave field obtained from the calculation. For example, if $\hat{\psi}(\omega, R)$ is the Fourier transform of the reduced velocity potential (RVP) at a given radius, R , then for a Voigt solid (Ewing, Jardetzky, and Press, 1957)

$$\hat{\psi}(\omega, R) = \hat{\psi}(\omega) e^{-\tau R} \quad (3.3)$$

where

$$\tau = \frac{1}{2} c \Delta r \frac{\omega^2}{\alpha^2} \quad (3.4)$$

$$\alpha \gg c \Delta r \omega \quad (3.5)$$

and $\hat{\psi}(\omega)$ is the elastic (distance invariant) RVP. Equations (3.3) and (3.4) can also be used to obtain a frequency dependent Q for the Voigt solid by recognizing that

$$e^{-\tau R} = e^{-\frac{\omega R}{2Q\alpha}} \quad (3.6)$$

Therefore,

$$Q = \frac{\omega}{2\tau\alpha} = \frac{\alpha}{c\omega\Delta r} \quad (3.7)$$

For the COWBOY and Grand Saline 200 pound yield calculations, we used the following parameters

$$c = 0.125$$

$$\alpha = 4,375 \text{ m/sec}$$

$$\Delta r = 0.25 \text{ m}$$

which, according to equations (3.4) and (3.7) gives

$$\tau = 3.223 \times 10^{-8} f^2 \quad (3.8)$$

$$Q = 2.23 \times 10^4 f^{-1} \quad (3.9)$$

with units of τ in meters and f in hertz. At a frequency of 100 hertz, we find that Q equals 223 and $\hat{\psi}(\omega, R)$ decreases by 4 percent between the "elastic" radius (17.83 meters) and 150 meters. Previous work has shown that a very low Q is required to produce the attenuation rates shown in Figures 16 through 19. Equation (3.9) does provide low Q s but at high frequencies. We find that in our 200 pound yield calculation that Q equals 40 at a frequency of 560 Hz and that at this frequency the RVP spectrum decreases by 75 percent between the elastic radius and 150 meters.

These results, while obtained for an artificial viscosity in order to show how to correct the calculated RVP for the viscosity, emphasize the importance of relating observed apparent attenuation to the frequencies which control the apparent attenuation. For example, the COWBOY data shown in Figures 16 through 19 show that attenuation in salt is severe for frequencies on the order of 500 hertz, something that should not surprise us. However, this data contains no information relevant to the issue of attenuation in the teleseismic frequency band.

For a more complete discussion of near-field attenuation models applied to COWBOY data, see Minster (1982). For our purposes it is sufficient to note that all RVP spectra calculated here for the Grand saline experiment involve viscoelastic attenuation given by equations (3.6), (3.8), and (3.9). These equations show that the computed RVP spectra can, for experimental purposes, be regarded as

elastic for frequencies less than about 125 hertz, assuming that the experiment will not be able to unambiguously resolve spectral RVP amplitude changes of 5 percent over a distance of 130 meters.

Figure 20 shows the RVP spectra for the two calculations at a yield of 200 pounds of Pelletol corresponding to Phase III of the Grand Saline tests. The difference in amplitude is a measure of the expected uncertainty due to choice of material properties for salt, in particular, the magnitude of Y_0 given in Table 1. Trulio (1978) has published an RVP spectra obtained by digitizing a velocity pulse, 63.4 meters from the 1,000 pounds COWBOY 11 event, which is beyond the scaled elastic radius we calculate for COWBOY. This spectra was shown scaled to the SALMON yield using an HE-nuclear equivalence relation, 2,000 pounds of Pelletol = 1.41 tons of nuclear energy. In order to compare our calculated spectra with this published spectra, we scaled our results to SALMON yield using the same scaling as reported by Trulio. Figure 21 compares the calculational results with the spectra from COWBOY 11, as published by Trulio. Good agreement between "measurement" and calculation was obtained at frequencies above 1 hertz. The local minimum in the COWBOY spectra at about 0.6 hertz may be an indication of either two-dimensional effects or an incomplete velocity pulse.

We present these results from our two calculations (peak velocities, peak displacements, and RVP spectra) as a prediction for the proposed 200 pound Pelletol event at the Grand Saline mine (Phase III). In the Appendix of this report, we present complete plots of velocity versus time at the same 14 ranges from the 200 pound event for each calculation. These may be interpolated to the actual guage locations or simply scaled to the detonated yield if different from 200 pounds of Pelletol.

In summary, we have normalized our computational constitutive models and material properties for salt to the ground motion from the SALMON, GNOME and COWBOY events. For our ground motion

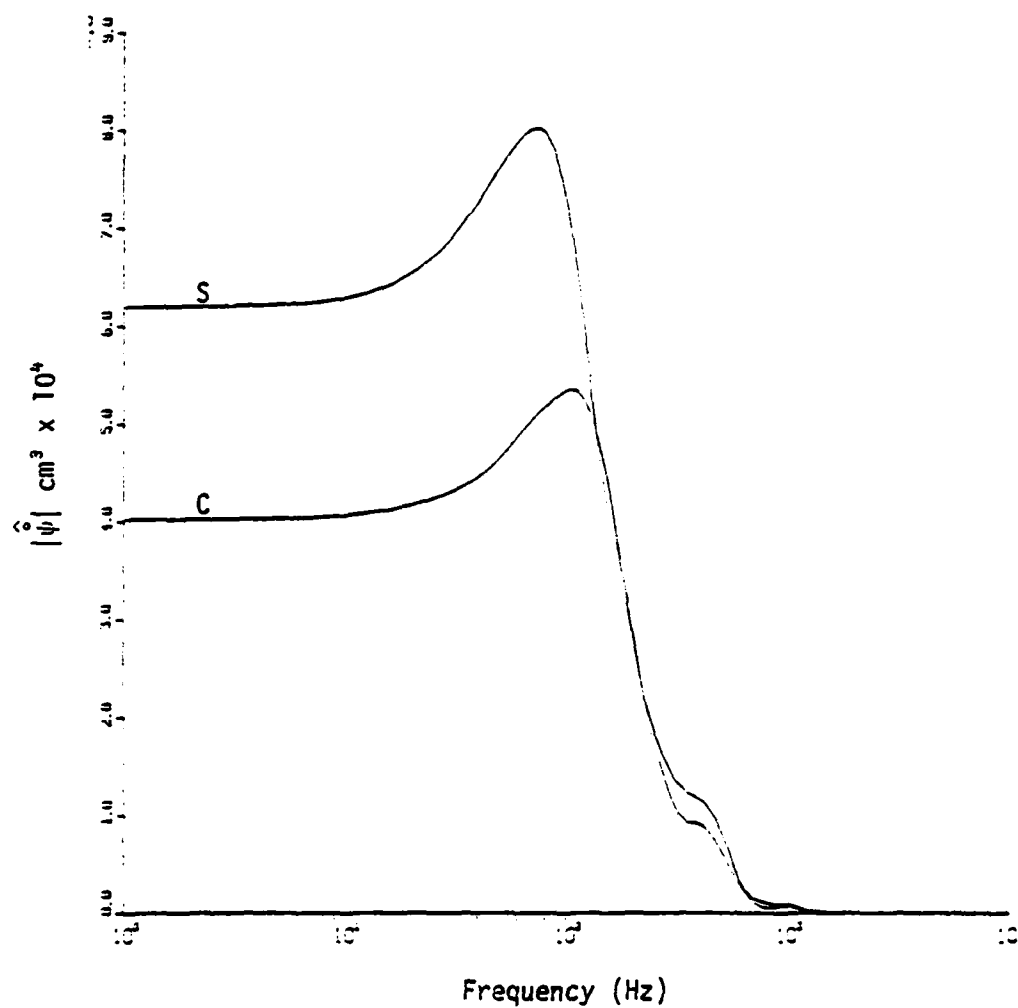


Figure 20. Computed RVP spectra at the elastic radii using SALMON material properties (S) and COWBOY properties (C) for a yield of 200 pounds of Pelletol.

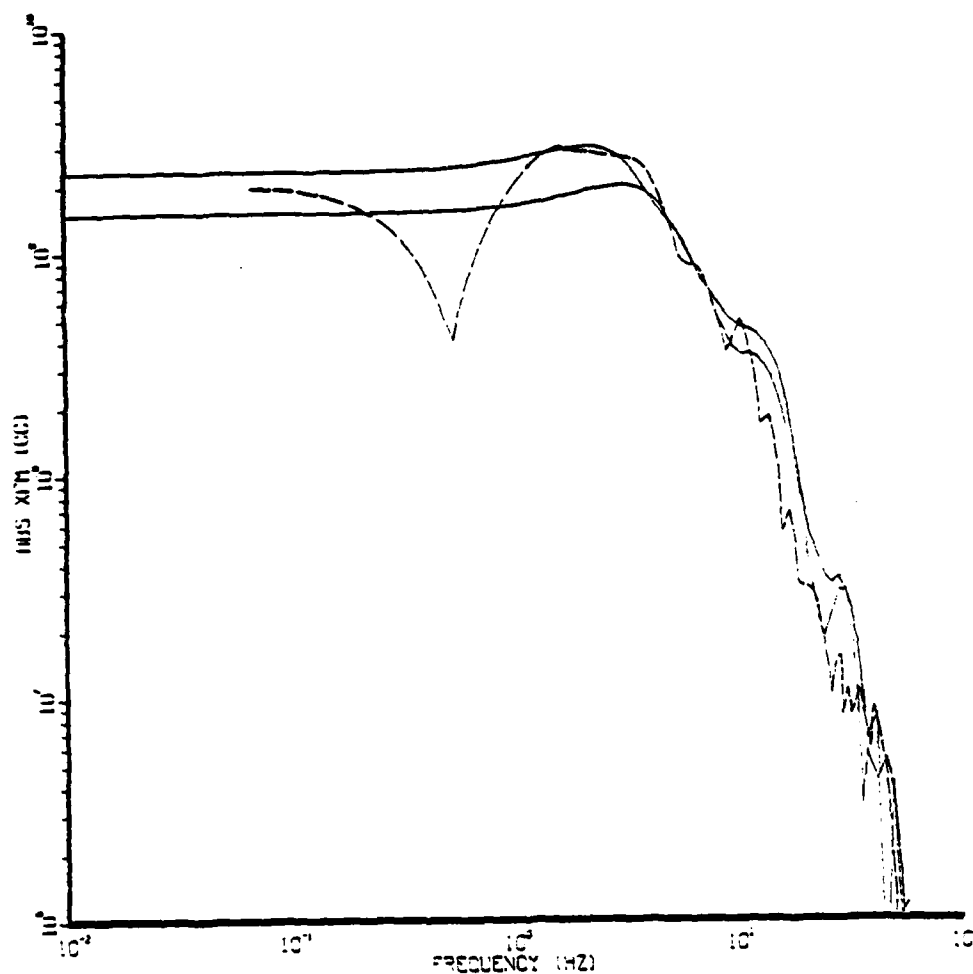


Figure 21. Calculated RVP spectra of Figure 20 simply scaled to SALMON yield (5.3 KT) compared to RVP spectra for gauge 2.4 - 15-V from COWBOY 11 (shown dotted) scaled to 5.3 KT by Trulio (1978) using HE-nuclear equivalence relation: 2,000 pounds of Pelletol = 1.41 tons of nuclear energy.

predictions for PHASE III of the Grand Saline experiments, we assumed that site material properties are similar to those of the normalizing events. Inelastic yielding is predicted by the finite difference calculations to occur out to a radius of from 17 to 23 meters for 200 pounds of Pelletol explosive. A cavity radius of 52 centimeters is anticipated. Bounding values of the RVP spectra, based on our uncertainty in Grand Saline material properties, are given in Figure 20.

IV. REFERENCES

- Cherry, J. T. and N. Rimer (1980), "A Constitutive Model for Salt," Systems, Science and Software's Executive Summaries submitted to VELA Seismological Center, Project VT/0712, Task 4.1.1, SSS-R-81-4725, July.
- Lee, E. L., J. R. Walton, and P. E. Kraner (1976), "Equation of State for the Detonation Products of Hexanitrostilbene at Various Charge Densities," Lawrence Livermore Laboratory Report, UCID 17134, May.
- Minster, J. B. (1982), "Effects of Linear and Nonlinear Attenuation for COWBOY," S-CUBED Internal Report (unpublished).
- Springer, D., M. Denny, J. Healy, and W. Mickey (1968), "The Sterling Experiment: Decoupling of Seismic Waves by a Shot-Generated Cavity," JGR, 73, pp. 5995-6010.
- Swift, L. M. (1963), "Project GNOME: Intermediate Range Earth Motion Measurements," PNE-111F.
- Trulio, J. G. (1978), "Simple Scaling and Nuclear Monitoring," Applied Theory, Inc. Final Report, ATR-77-45-2, April.

APPENDIX

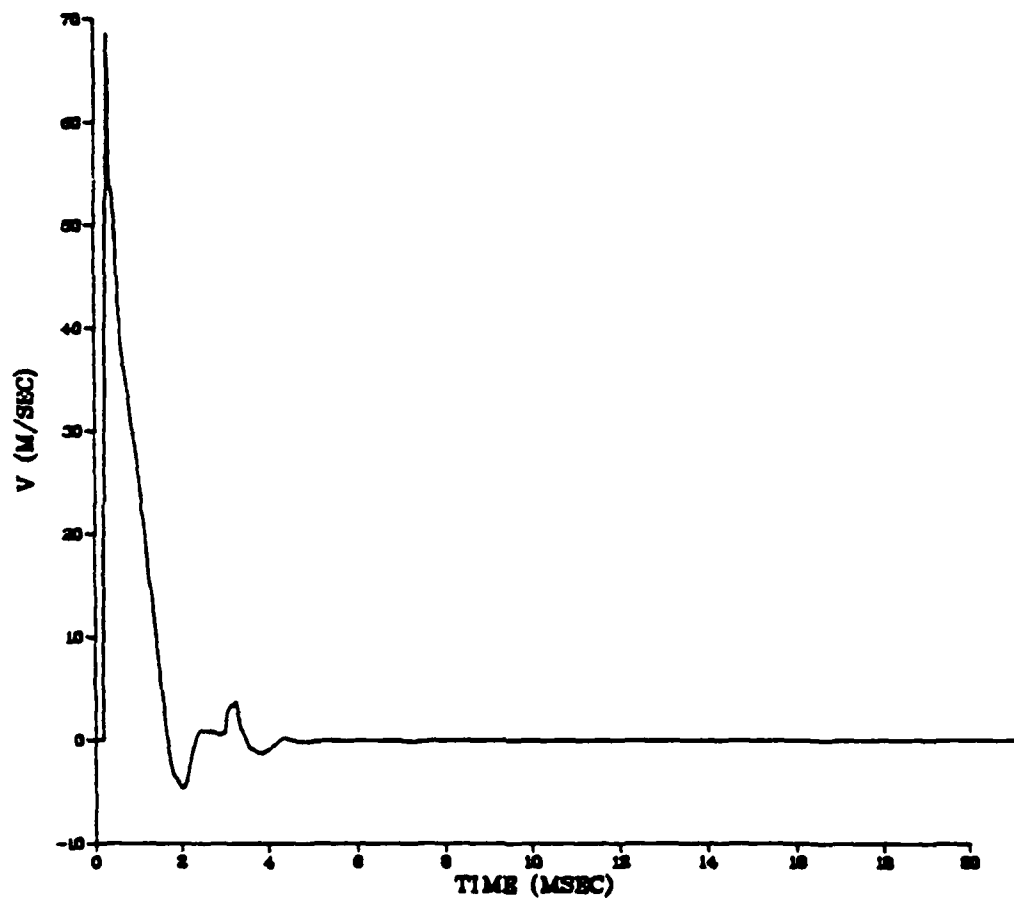
APPENDIX

In this Appendix we present plots of velocity versus time from two predictive calculations of 200 lb Pelletol events in the Grand Saline Salt Dome. Salt Run 603 refers to a calculation made using SALMON material properties and Salt Run 588 refers to calculations using COWBOY material properties. Each plot label shows the range, R, in meters, and the maximum and minimum velocities calculated at that range. The spike in the negative pulses (at approximately 3 msec for a range of 1.1 m) is due to the opening and subsequent closure of a tensile crack at a range of 1.0 m. This crack signal, which may or may not have physical significance, did impact the pulses at all other ranges.

SALT RUN 603

R= 1083+000 METERS

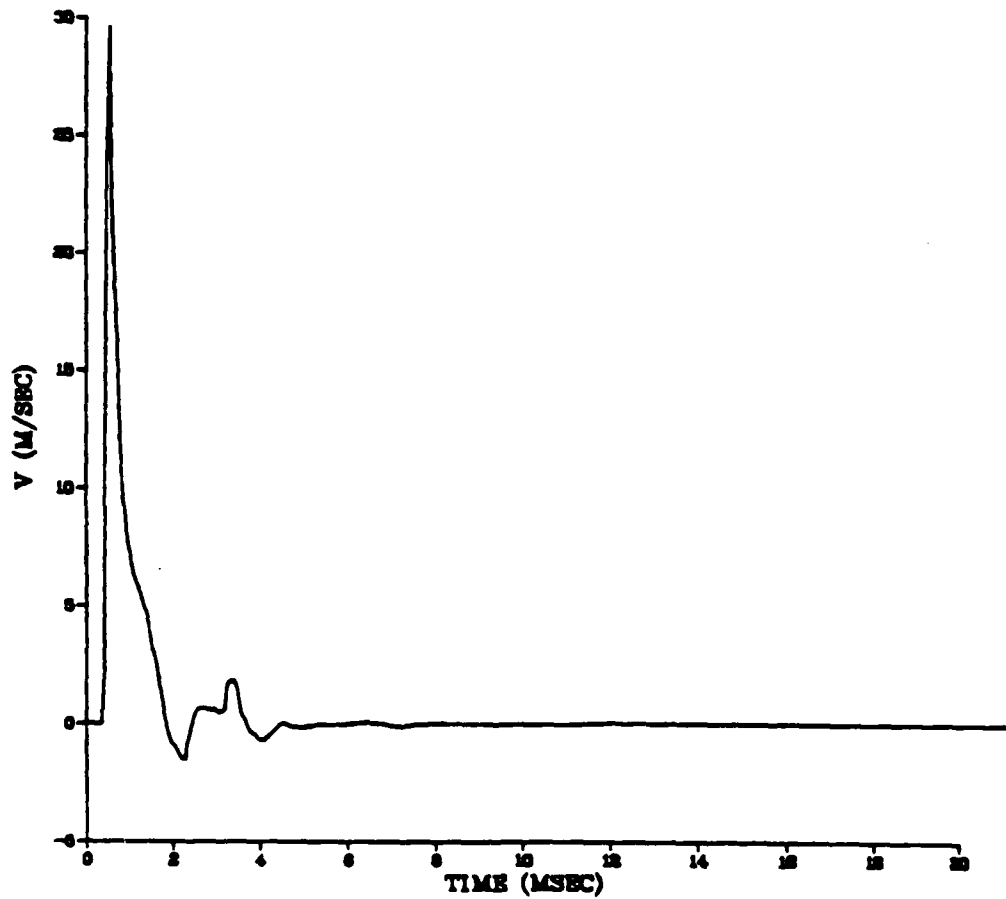
YMIN=-4.727+000 YMAX= 6.857+001



SALT RUN 603

R= 1.919+000 METERS

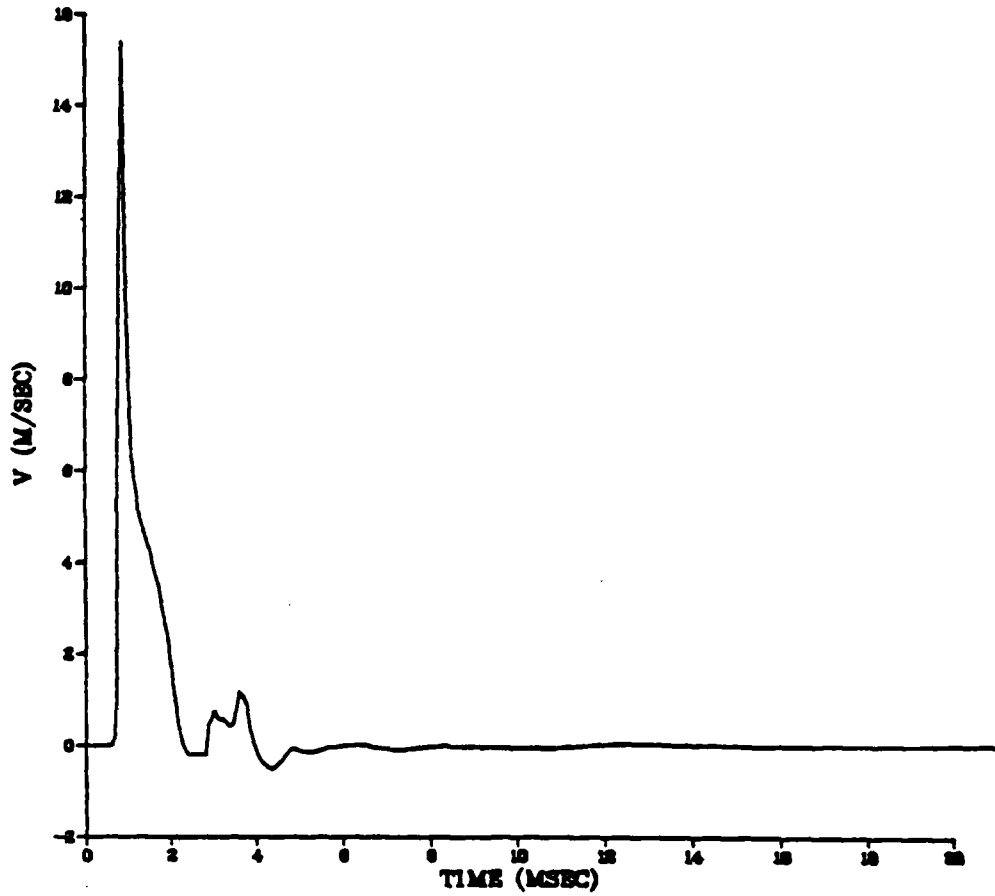
YMIN=-1.529+000 YMAX= 2.939+001



SALT RUN 603

R= 3314+000 METERS

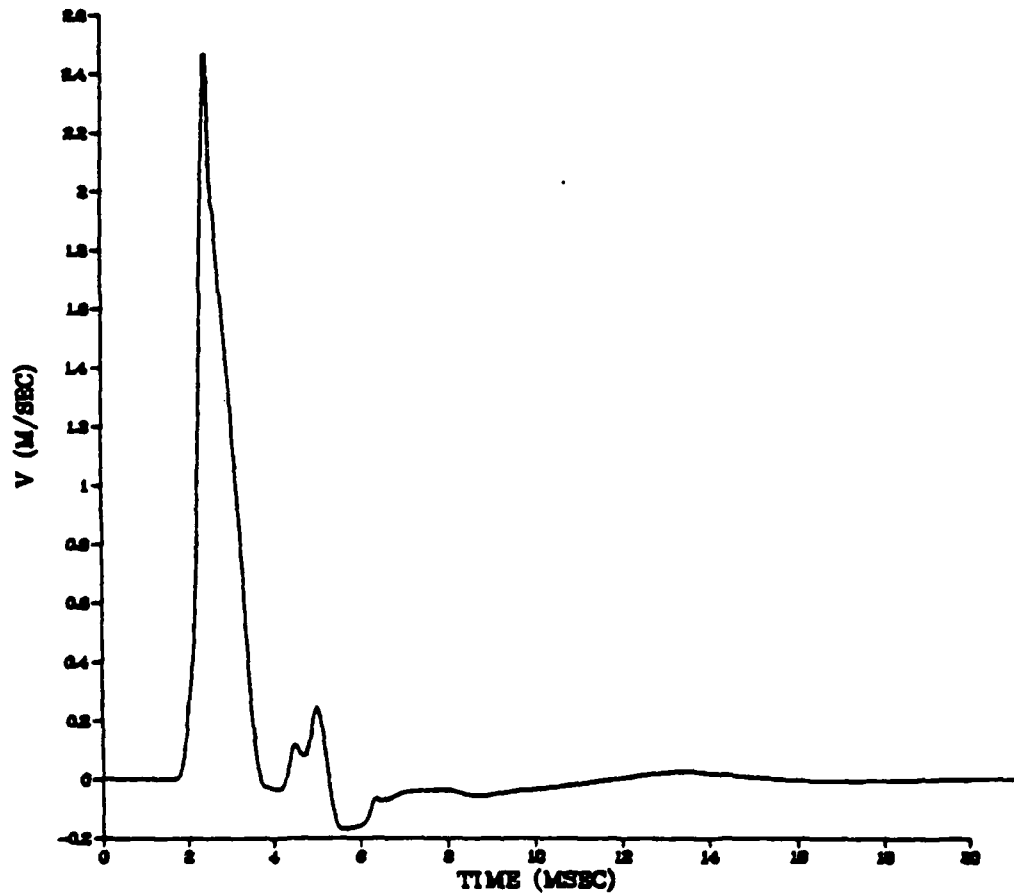
YMIN=-5241-001 YMAX= 1538+001



SALT RUN 603

R= 8.832+000 METERS

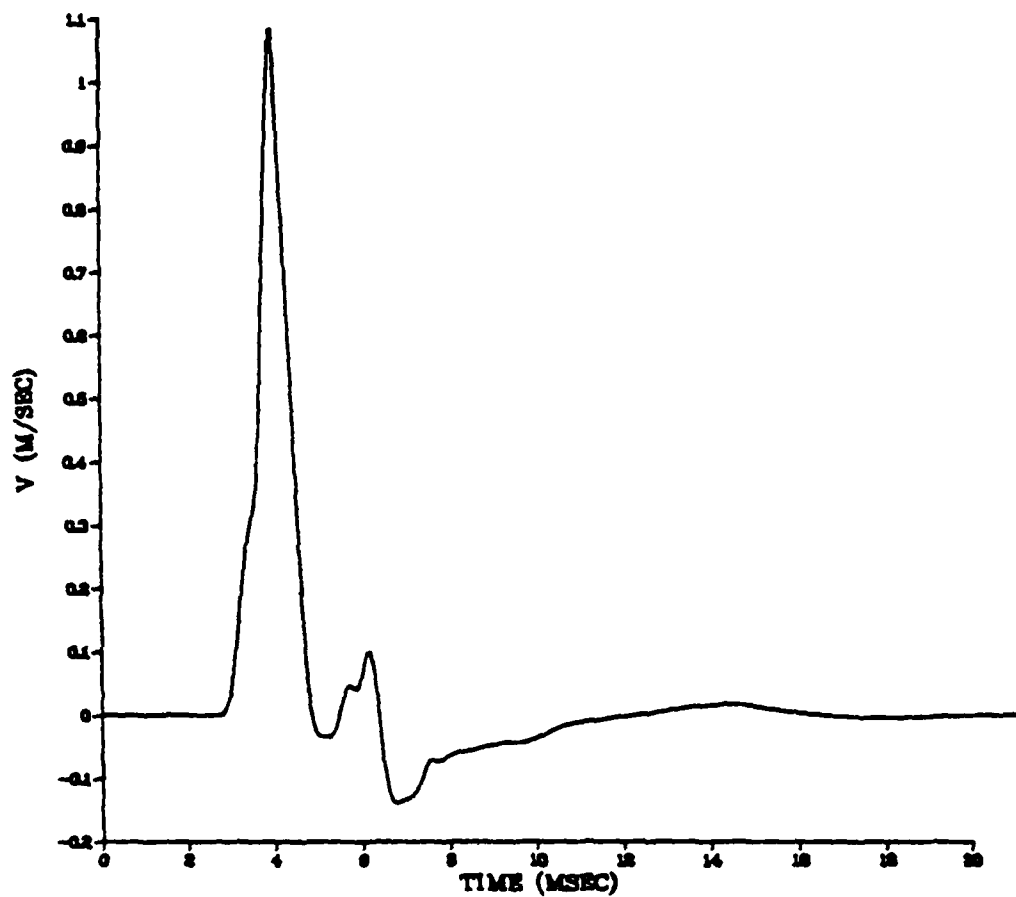
YMIN=-1.719-001 YMAX= 2.467+000



SALT RUN 603

R= 1408+001 METERS

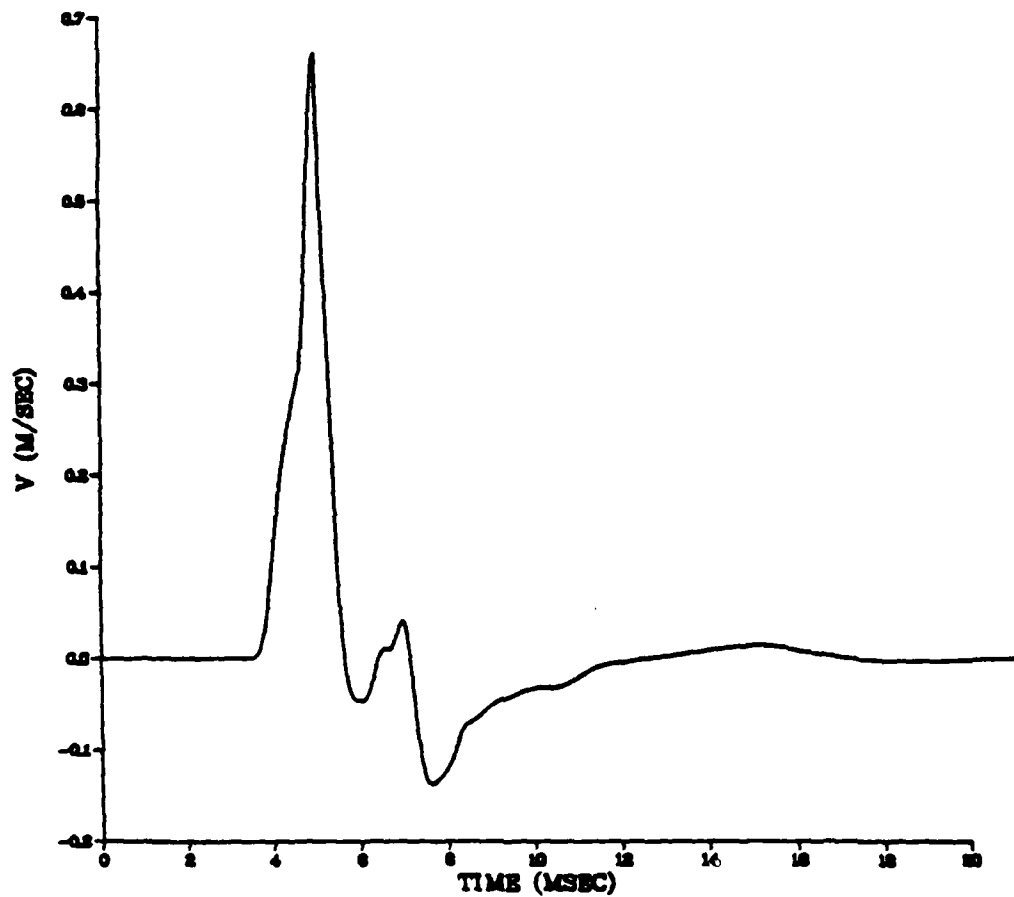
YMIN=-1387-001 YMAX= 1084+000



SALT RUN 603

R= 1.783+001 METERS

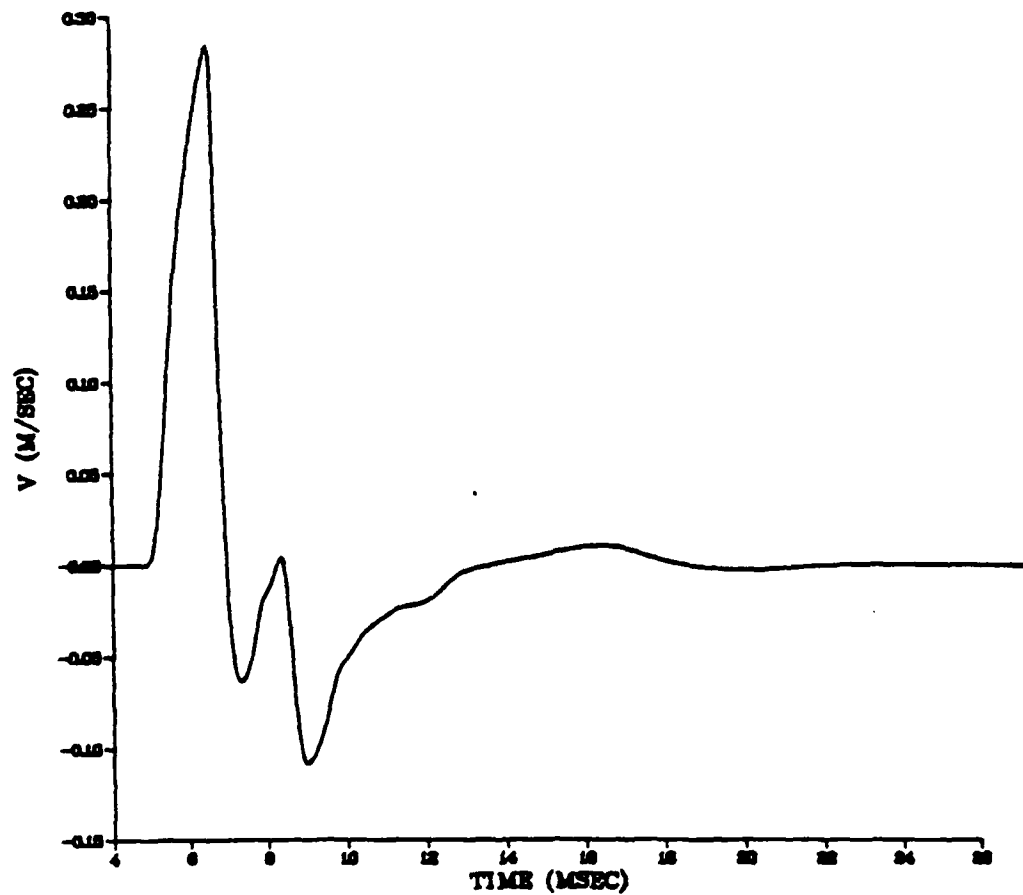
YMIN=-1.380-001 YMAX= 6.612-001



SALT RUN 603

R= 2408+001 METERS

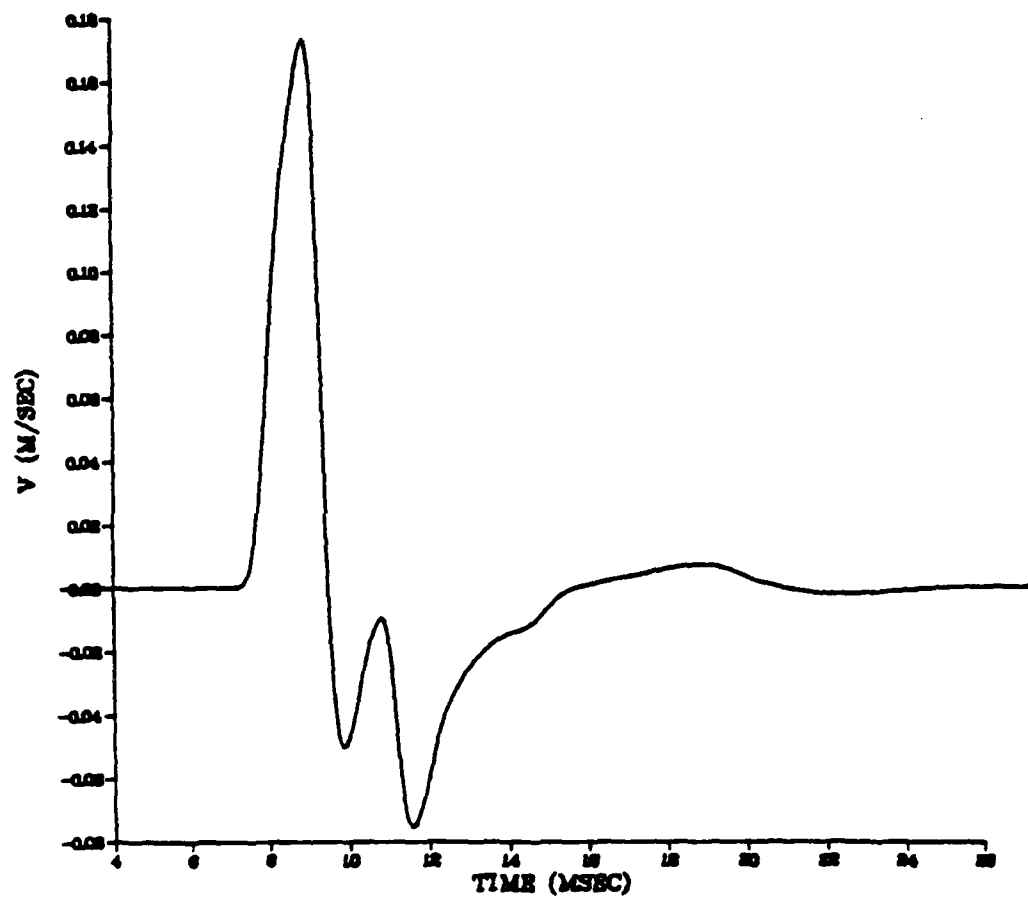
YMIN=-1085-001 YMAX= 2840-001



SALT RUN 603

R= 3558+001 METERS

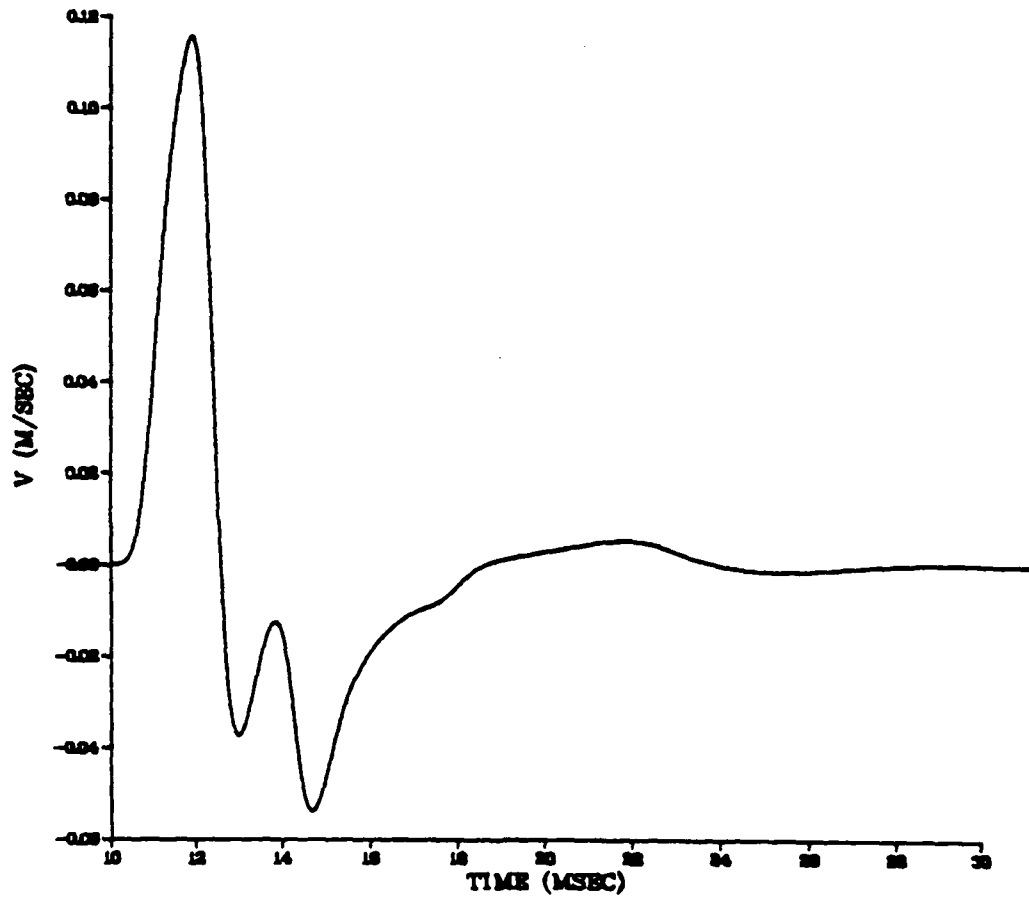
YMIN=-7548-002 YMAX= 1735-001



SALT RUN 603

R= 4.958+001 METERS

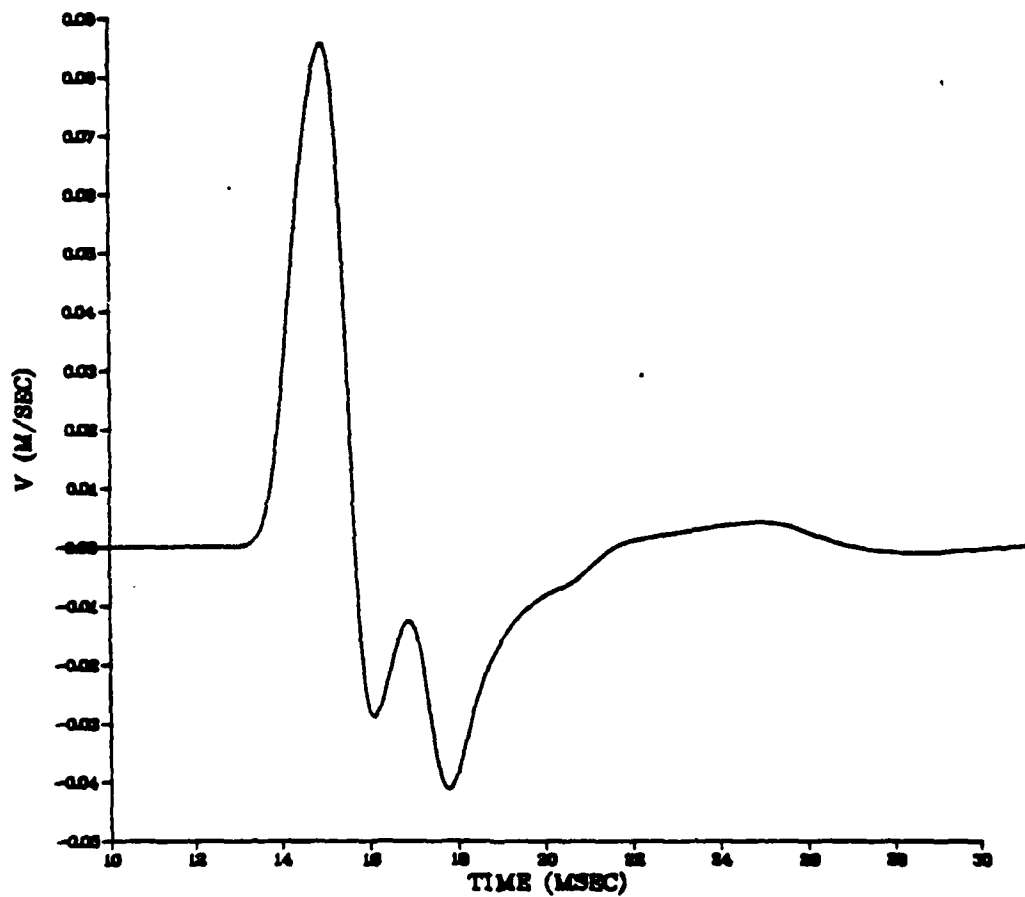
YMIN=-5.387-002 YMAX= 1.157-001



SALT RUN 603

R= 8.358+001 METERS

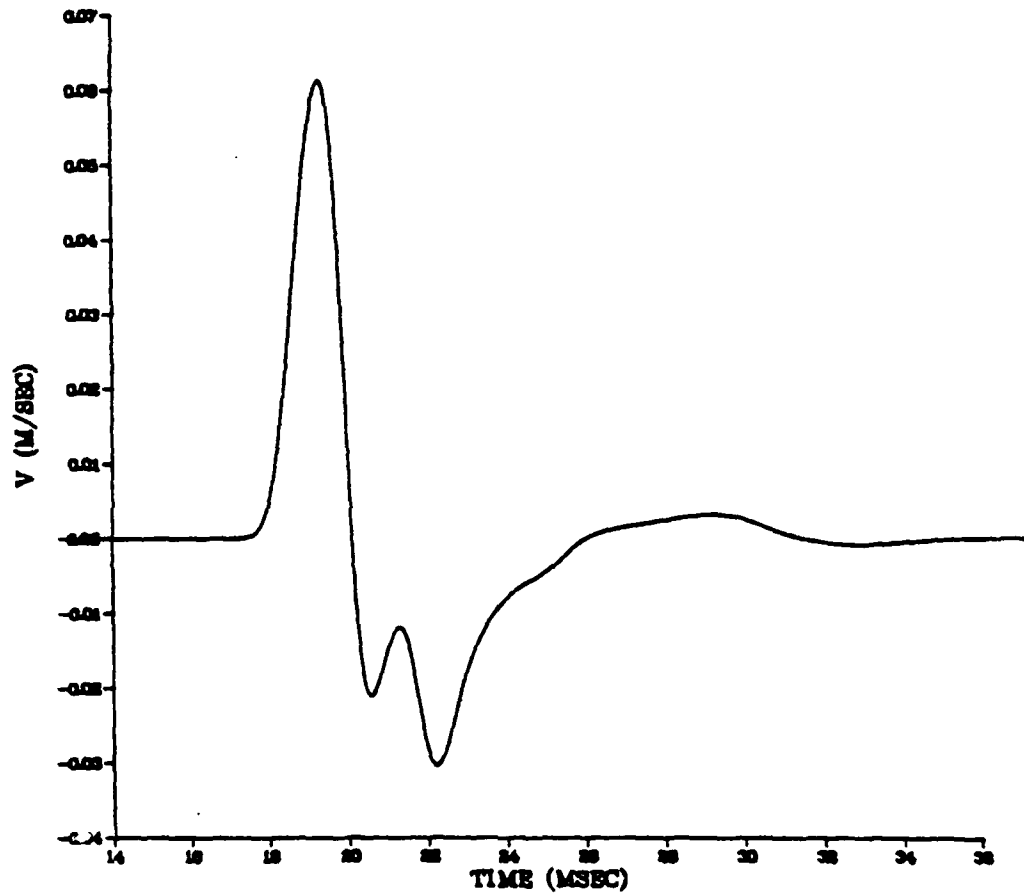
YMIN=-4.130-002 YMAX= 8.563-002



SALT RUN 603

R= 8.358+001 METERS

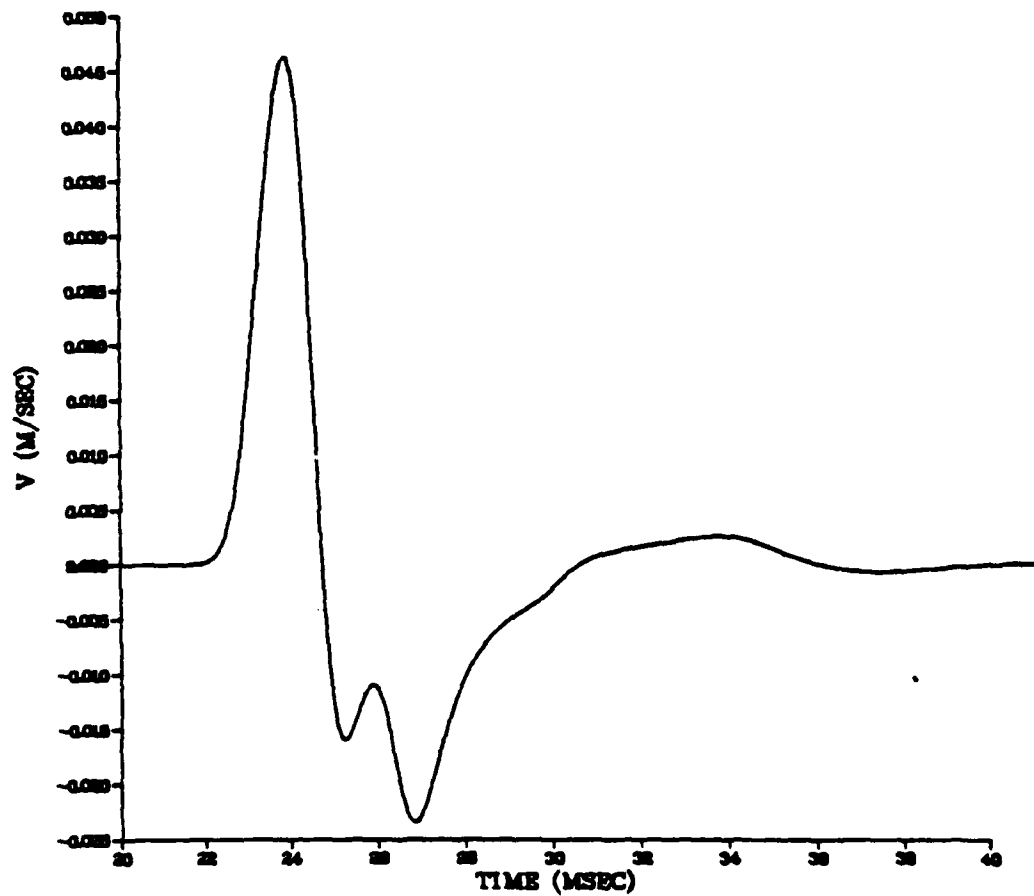
YMIN=-3.042-002 YMAX= 6.127-002



SALT RUN 603

R= 1.048+002 METERS

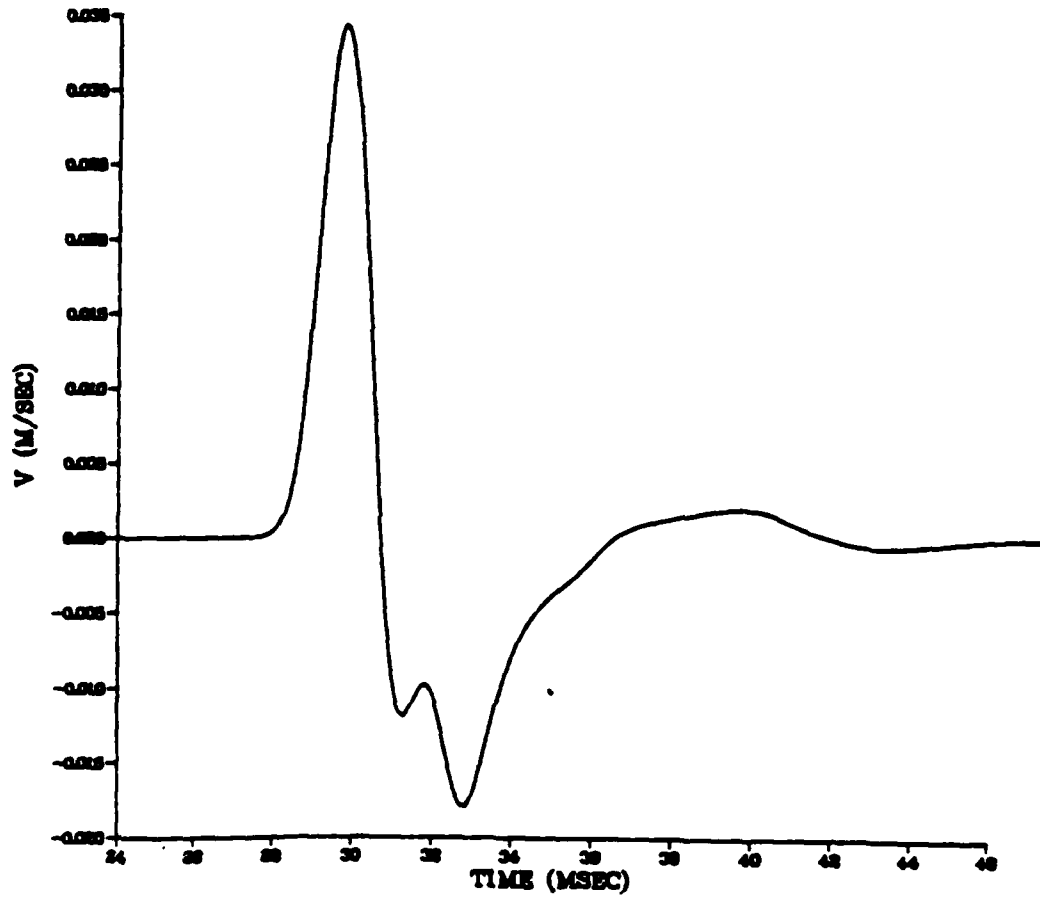
YMIN=-2.351-002 YMAX= 4.827-002



SALT RUN 603

R= 1.316+002 METERS

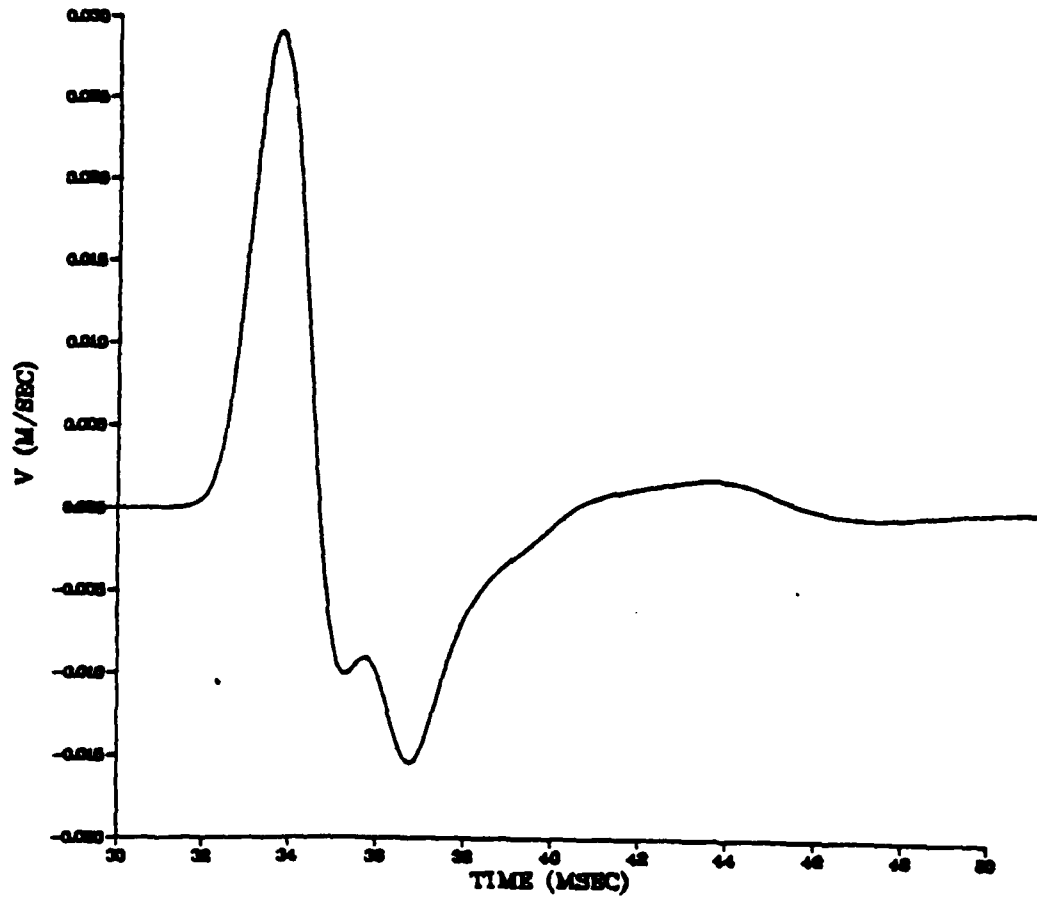
YMIN=-1.786-002 YMAX= 3.444-002



SALT RUN 603

R= 1499+002 METERS

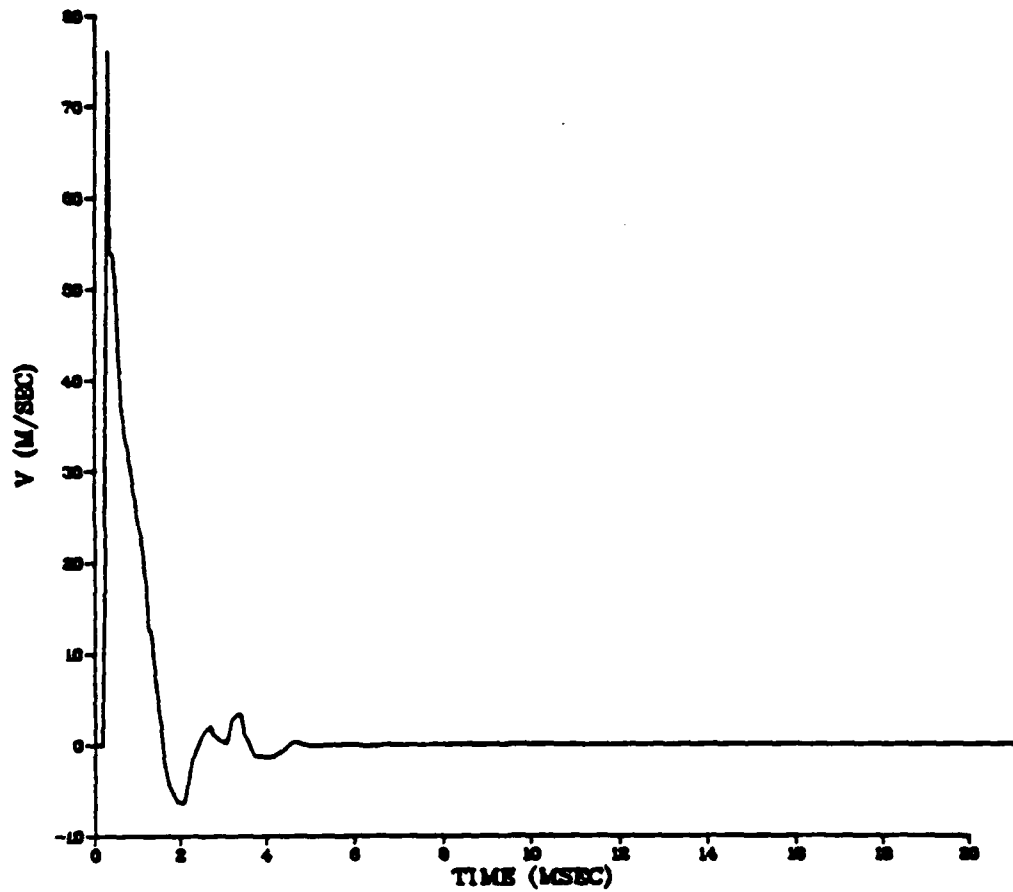
YMIN=-1549-002 YMAX= 2905-002



SALT RUN 588

R= 1.083+000 METERS

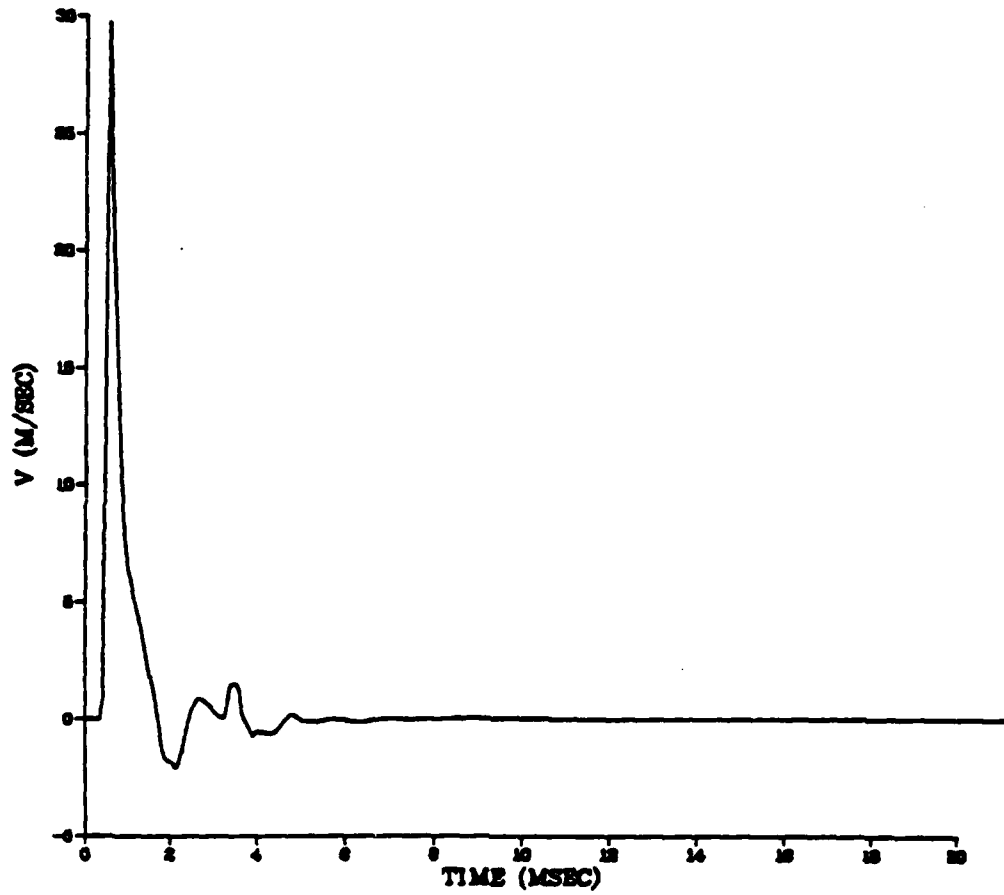
YMIN=-6.452+000 YMAX= 7.612+001



SALT RUN 588

R= 1.919+000 METERS

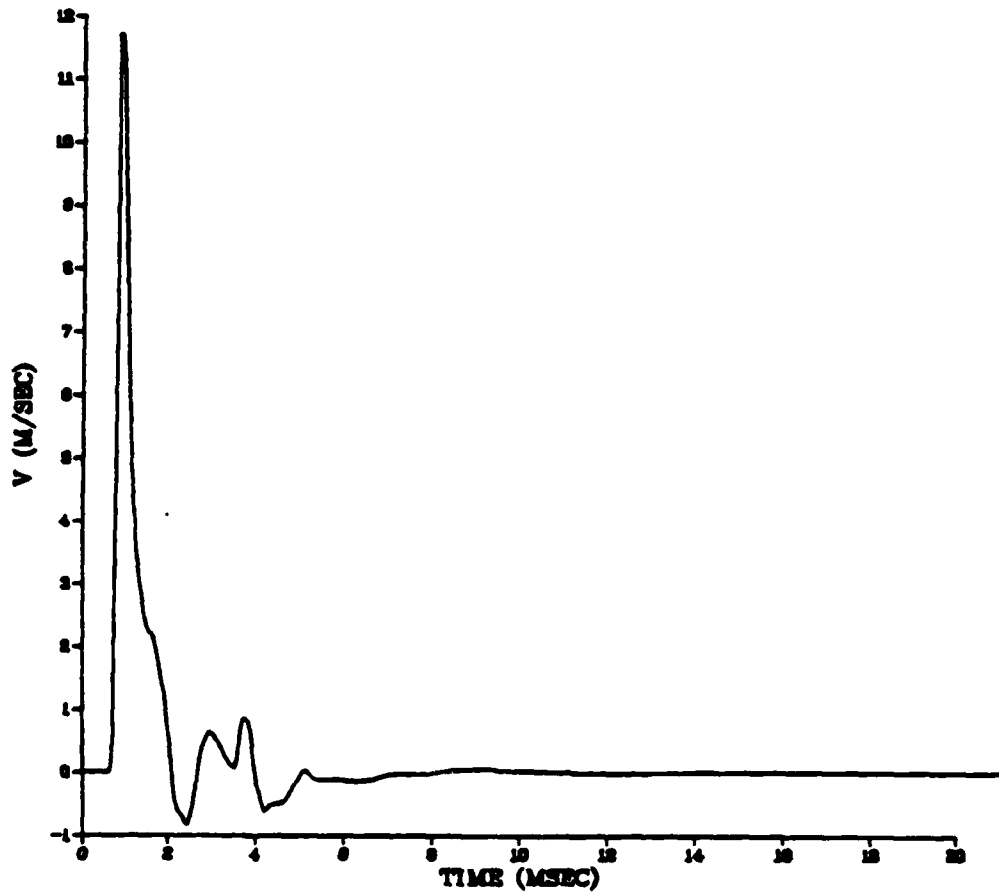
YMIN=2.053+000 YMAX= 2.972+001



SALT RUN 588

R= 3.314+000 METERS

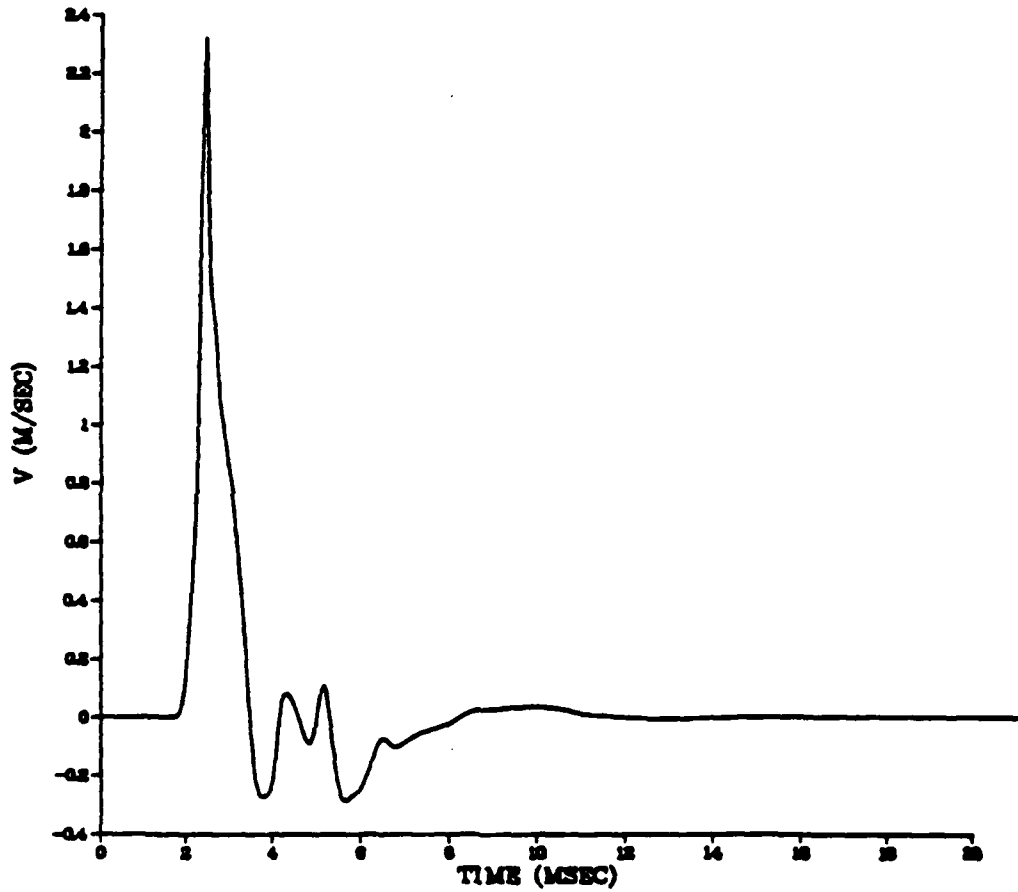
YMIN=-8.398-001 YMAX= 1.71+001



SALT RUN 588

R= 8.832+000 METERS

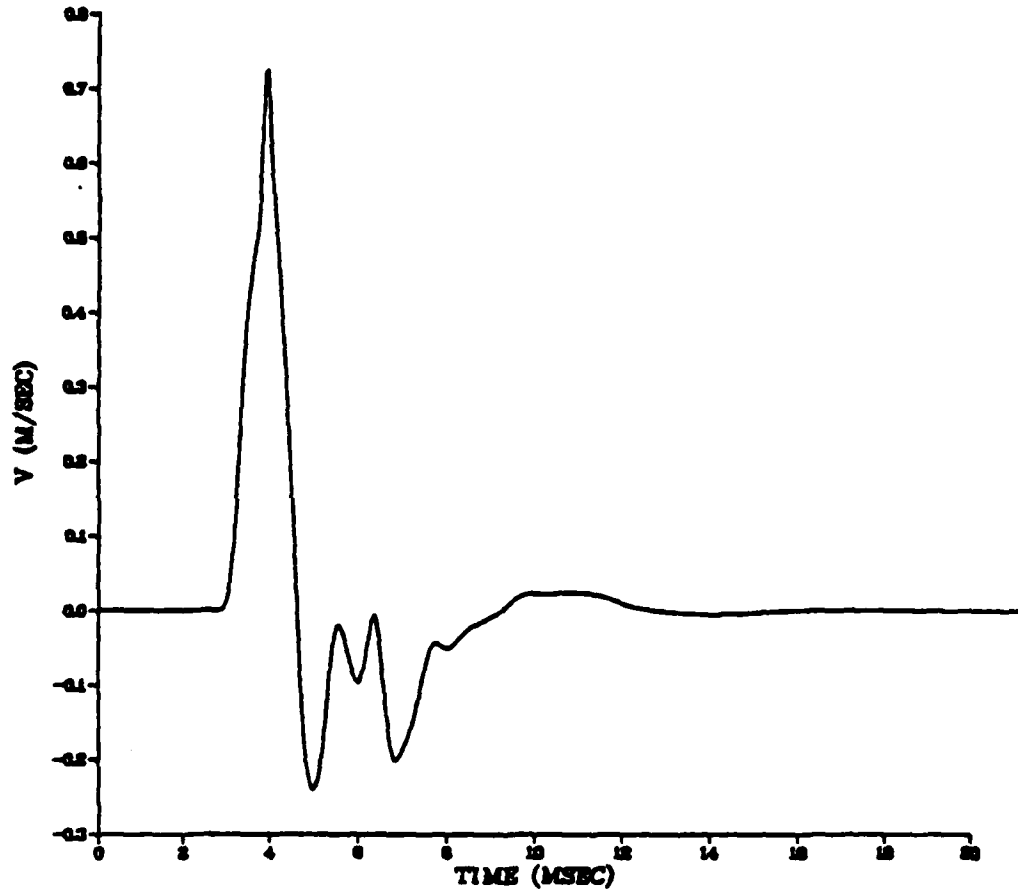
YMIN=-2.908-001 YMAX= 2.322+000



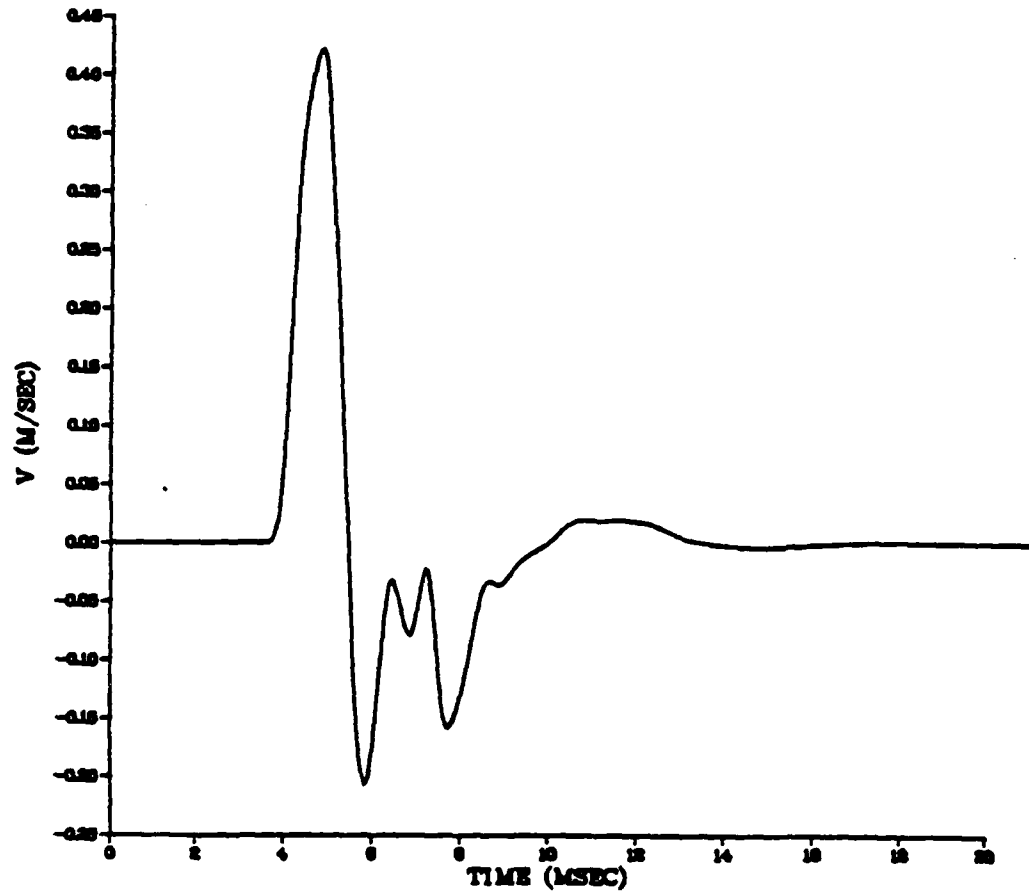
SALT RUN 588

R= 1408+001 METERS

YMIN=-2407-001 YMAX= 7244-001



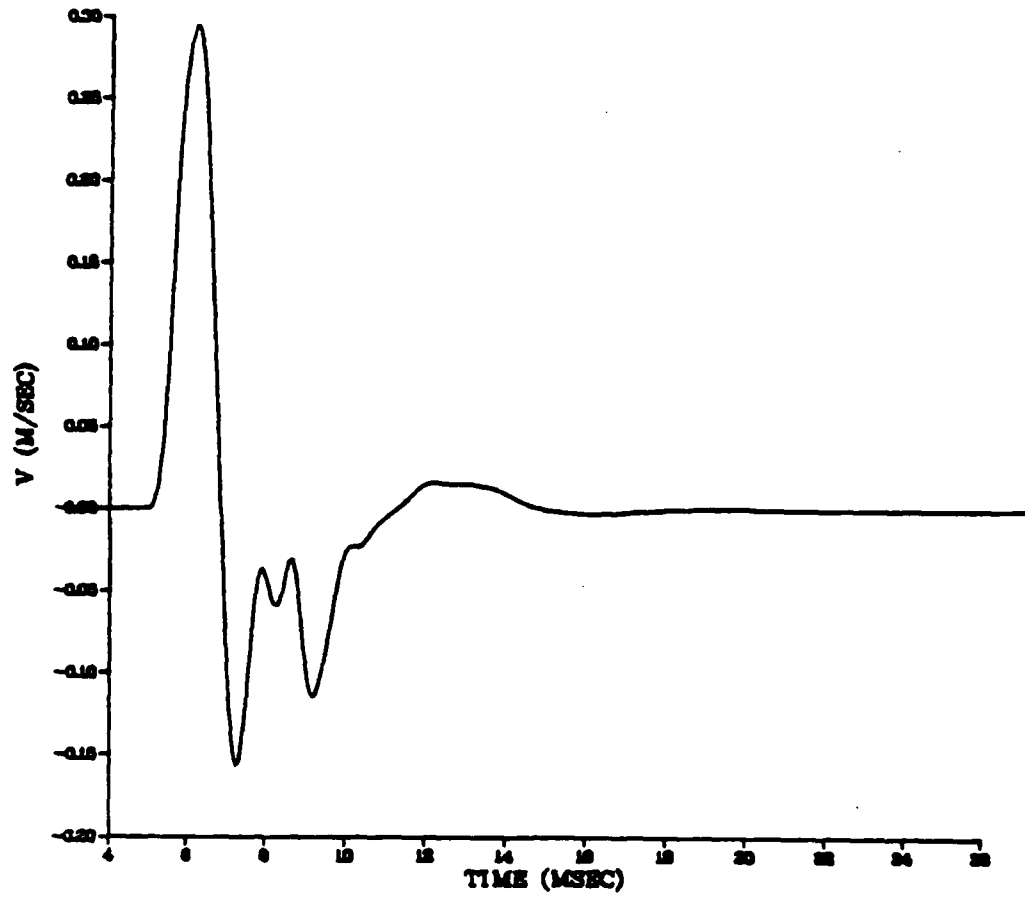
SALT RUN 588
R= 1.783+001 METERS
YMIN=-2.089-001 YMAX= 4.225-001



SALT RUN 588

R= 2.408+001 METERS

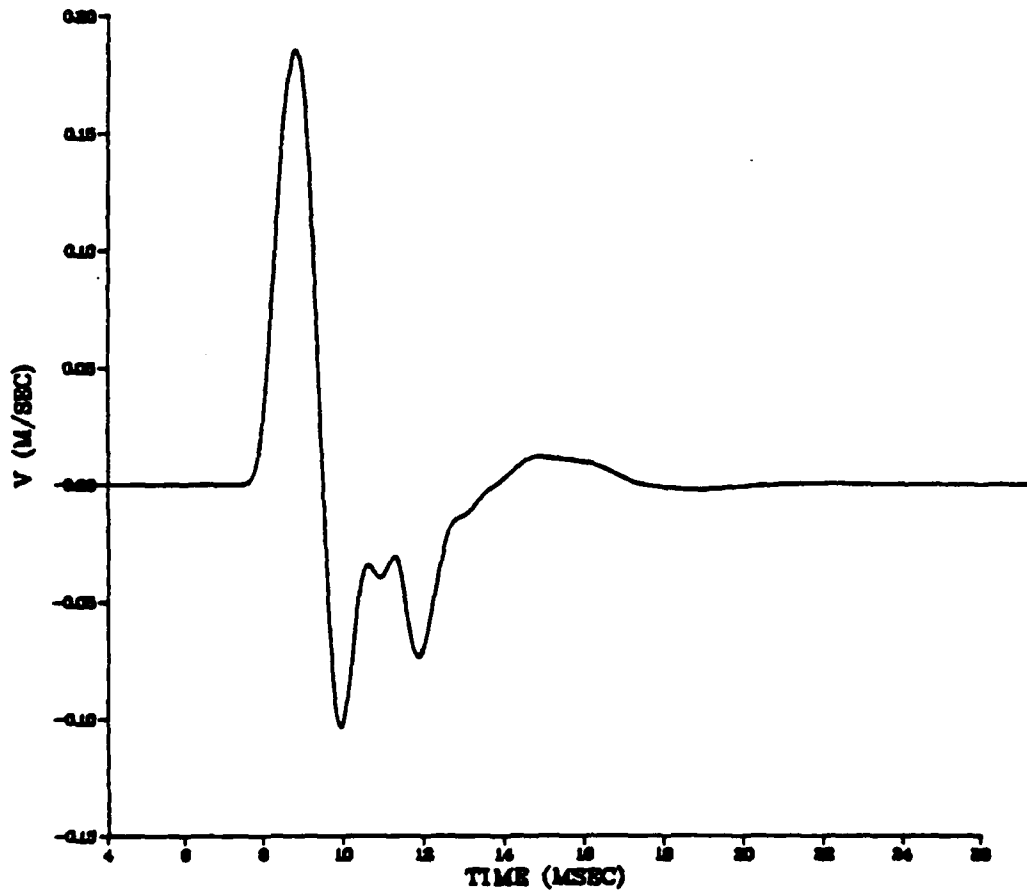
YMIN=-1.571-001 YMAX= 2.942-001



SALT RUN 588

R= 3.558+001 METERS

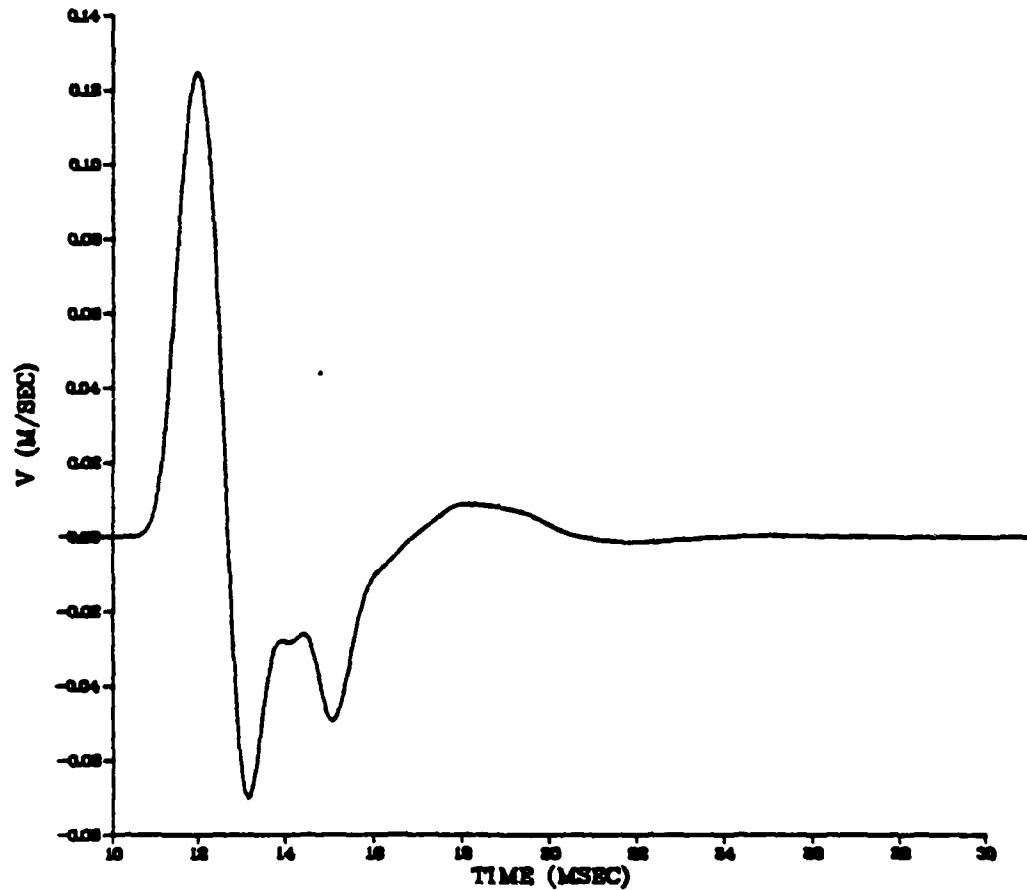
YMIN=-1.037-001 YMAX= 1.833-001



SALT RUN 588

R= 4.000+001 METERS

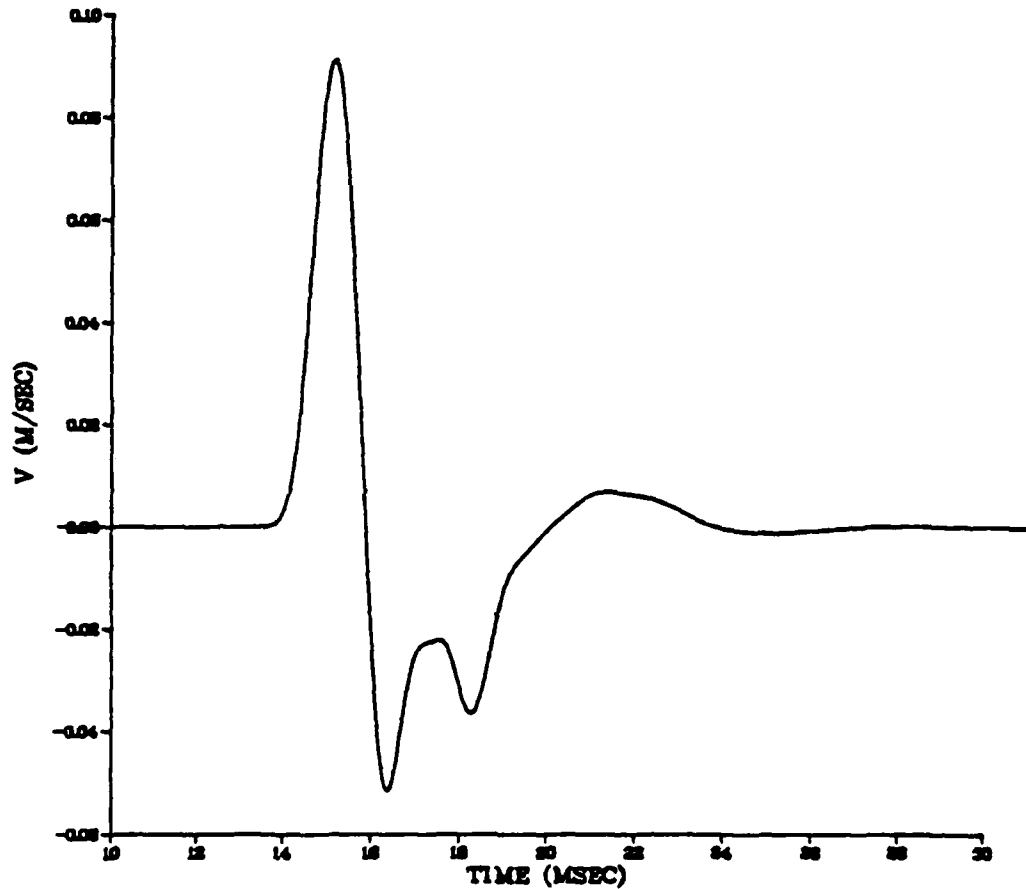
YMIN=-7.041-002 YMAX= 1.245-001



SALT RUN 588

R= 8.358+001 METERS

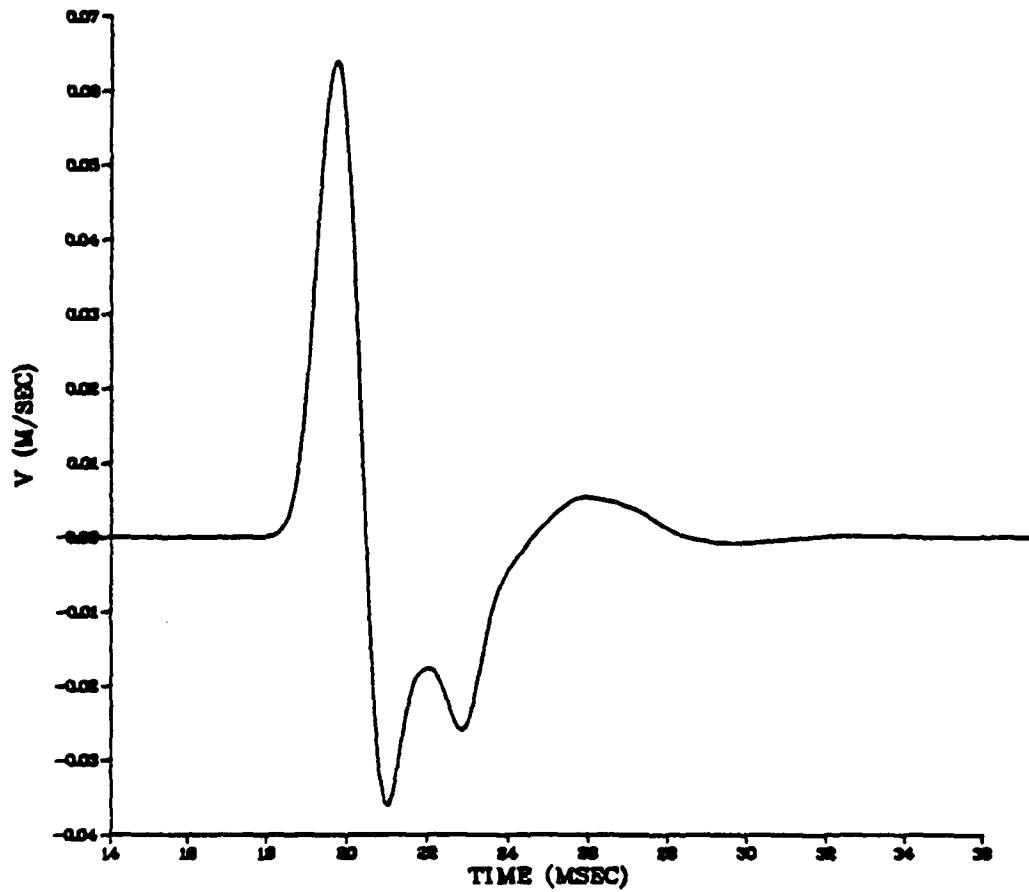
YMIN=-5.164-002 YMAX= 8.132-002



SALT RUN 588

R= 8.358+001 METERS

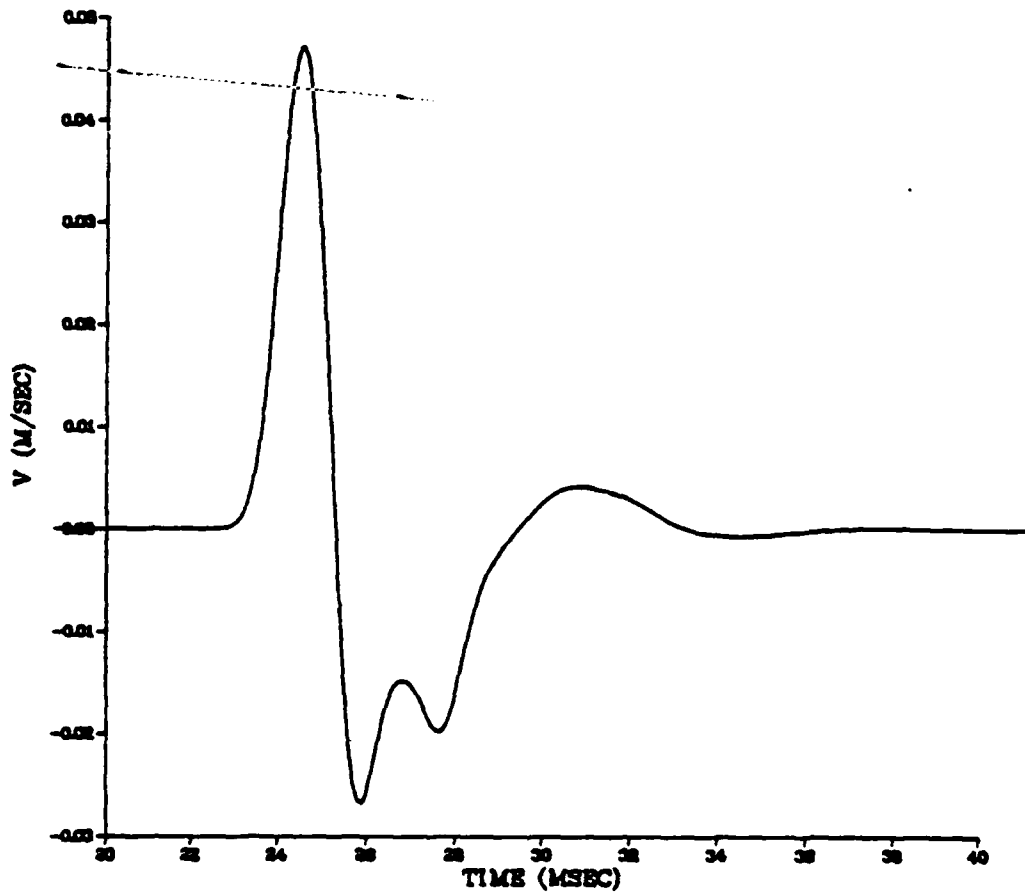
YMIN=-3.621-002 YMAX= 8.401-002



SALT RUN 588

R= 1.046+002 METERS

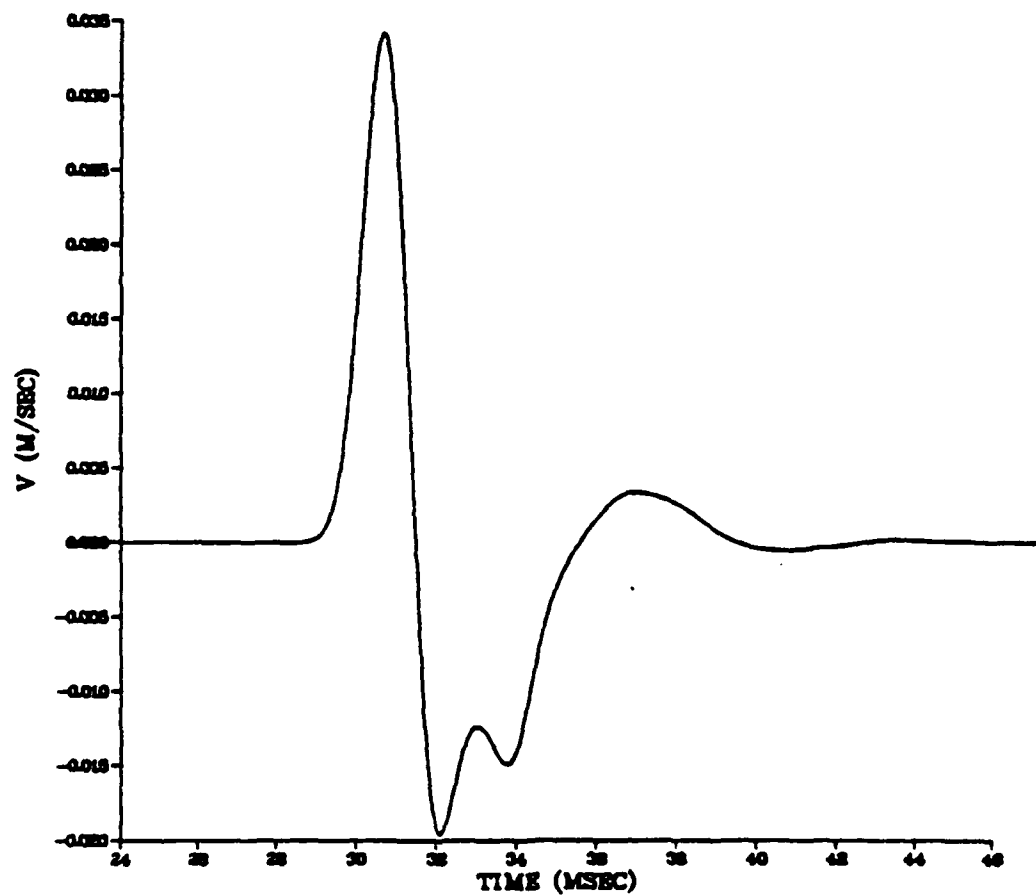
YMIN=-2.680-002 YMAX= 4.723-002



SALT RUN 588

R= 1.316+002 METERS

YMIN=-1.962-002 YMAX= 3.421-002



SALT RUN 588

R= 1.496+002 METERS

YMIN=-1.847-002 YMAX= 2.842-002

